Design of chord sidewall failure in RHS joints using steel grades up to S960

Lan, Xiaoyi; Wardenier, Jaap; Packer, Jeffrey A.

DOI
10.1016/j.tws.2021.107605

Publication date
2021

Document Version
Accepted author manuscript

Published in
Thin-Walled Structures

Highlights

- Up-to-date reported test and numerical results of chord sidewall failure in RHS joints were collated.
- Effects of brace-to-chord height ratio, brace angle, steel grade and chord stress ratio were evaluated.
- Two design methods were proposed for chord sidewall failure in RHS joints under brace axial compression.
- Design of chord sidewall failure in RHS joints under brace axial tension and brace bending was discussed.

Design of chord sidewall failure in RHS joints using steel grades up to S960

Xiaoyi Lan [a,*], Jaap Wardenier [b], Jeffrey A. Packer [c]

[a] School of Civil and Environmental Engineering, Nanyang Technological University, Singapore
[b] Department of Engineering Structures, Delft University of Technology, The Netherlands
[c] Department of Civil & Mineral Engineering, University of Toronto, Canada

*Corresponding author, Email address: xiaoyi.lan@ntu.edu.sg

Abstract: It is well known that the current design rules adopted by international design codes such as ISO 14346 and design guides, e.g., the CIDECT design guide No. 3, for chord sidewall failure in mild steel RHS joints under brace axial compression are considerably conservative, if the RHS joints are adequately supported out-of-plane. This paper presents an investigation into chord sidewall failure in rectangular hollow section (RHS) joints using steel grades up to S960. Representative existing design methods for chord sidewall failure in RHS joints are reviewed, and two alternative design methods, i.e., the modified bearing-buckling method and the Lan-Kuhn method, are proposed. Up-to-date test and numerical results reported in the literature are compiled. A wide range of geometric parameters, steel grades up to S960 and loading cases of brace axial loading, brace in-plane bending and brace out-of-plane bending are covered. The existing and proposed design methods are assessed against the collated results. The effects of brace-to-chord height ratio, brace angle, steel grade and chord stress ratio are evaluated. It is shown that the proposed design methods can provide more consistent resistance predictions for chord sidewall failure in mild steel and high-strength steel RHS joints under brace axial compression. Corresponding user-friendly design rules are suggested. The design of chord sidewall failure in RHS joints under brace axial tension, brace in-plane bending and brace out-of-plane bending is discussed. Further required research on, in particular, high-strength steel RHS joints is highlighted.

Keywords: Rectangular hollow section; X joints; T joints; Y joints; Chord sidewall failure; Design rules

1. Introduction

Rectangular hollow sections (RHS) exhibit an aesthetic appearance and feature excellent structural efficiency especially with regard to loading of compression and torsion because of the closed shape. The evident advantages of RHS result in wide applications in structural, mechanical, transport and offshore fields. The connection of RHS members is vitally crucial for the structural integrity, and direct welding of the intersecting brace to the through chord is the simplest and cleanest solution for the connection. Design rules are needed for such welded RHS joints to facilitate structural applications.

Fig. 1 shows the configurations and notations of RHS-to-RHS X, T and Y joints. Chord sidewall failure is a typical failure mode in full-width RHS joints with brace-to-chord width ratio (β) of 1.0. In the 1970s, test data for chord sidewall failure in RHS X joints became available from Czechowski and Brodka [1] and Barentse [2]. Czechowski and Brodka [1] developed an empirical equation based on their data which showed a large scatter. This is probably because in the Polish tests the brace and chord of the X joints were fabricated from cold-formed channel sections with fabrication tolerances. Furthermore, distortion of the chord cross-section resulted in a sway-type failure mode because of the pinned-end support at the brace ends and the inadequate out-of-plane support at the chord ends. Barentse [2] assessed various local buckling models against his test results. Brodka and Szlendak [3] and Kato and Nishiyama [4] proposed analytical models which appear to be too complicated for design. Later, Wardenier and Davies [5] developed a simpler combined bearing-buckling model based on a conservative lower bound of the aforementioned Polish and Dutch test results. It adopts a combined check for the bearing resistance using the steel yield stress of the chord (f_{y0}) and the local buckling capacity employing a local buckling stress of the chord sidewall (f_k). The value of f_k can be determined using the relevant Eurocode buckling curves [6] or equivalent buckling curves. The bearing-buckling method is adopted by various design codes, e.g., EN 1993-1-8 [7] and ISO 14346 [8], and design guides such as the CIDECT design guide No. 3 [9-10] and the IIW recommendations [11-13] for chord sidewall failure.

Extensive research on chord sidewall failure has been conducted since the mid-1980s. Davies et al. [14] summarised various design methods and the influence of different joint parameters for chord sidewall failure in RHS X joints. Packer [15] conducted tests on 31 full-width RHS X joints to supplement the existing test database of 40 RHS X joints reported in the literature, and concluded that the codified bearing-buckling method for chord sidewall failure was too conservative. Giddings and Wardenier [16] compiled CIDECT Monograph No. 6 in which various state-of-the-art theories at that time for chord sidewall failure were summarised. Davies and Roodbaraky [17] examined the effect of brace angle (θ_1) on the resistances of various failure modes in RHS X joints using the results of tests as well as elastic and elastic-plastic numerical analyses reported by Platt [18]. It was found that the average resistance enhancement for decreasing brace angles could be quantified by the brace angle function of $(1/\sin\theta_1)^{0.5}$ for chord sidewall failure in RHS X joints under brace axial compression and tension. Yu [19] proposed a four-hinge yield line model and assumed that the chord sidewall was fully clamped for chord sidewall failure in RHS-to-RHS X and T joints subjected to brace axial compression, brace in-plane bending and brace out-of-plane bending. Becque and Cheng [20] conservatively assumed that the chord sidewall is pinned along the chord length direction, and proposed a plate buckling model to predict the buckling initiation of the chord sidewall in RHS-to-RHS X joints. Kuhn et al. [21] proposed an equation of the buckling reduction factor which is linearized against chord height to wall thickness ratio ($2\gamma^*=h_0/t_0$) for chord sidewall failure in RHS X joints under brace axial compression. This simplifies the determination of f_k values without using the buckling curves. Wardenier [22] proposed to modify the codified resistance equation to consider the effect of brace-to-chord height ratio ($\eta^*=h_1/h_0$). Lan et al. [23-24] developed an analytical model for plate buckling to properly consider the beneficial restraint of the chord face and brace for the chord sidewall in RHS-to-RHS X and T joints. Comprehensive assessment of the design methods remains limited, and more suitable design rules for chord sidewall failure in RHS joints are needed.

This study aims to evaluate existing design methods and to propose suitable design methods and design rules for chord sidewall failure in mild steel and high-strength steel RHS joints. Test and numerical results of RHS X and T joints reported in the literature have been collated. A wide range of geometric parameters, steel grades up to S960 and loading cases of brace axial loading, brace in-plane bending and brace out-of-plane bending were covered. Existing design methods and proposed design methods in this study were assessed against the compiled results. The effects of brace-to-chord height ratio, brace angle, steel grade and chord stress were evaluated. Design rules were proposed for chord sidewall failure in mild steel and high-strength steel RHS joints under brace axial compression. The design of chord sidewall failure in RHS joints under brace axial tension, brace in-plane bending and brace out-of-plane bending was discussed. Further research on, in particular, high-strength steel RHS joints was highlighted.

2. Design methods for chord sidewall failure

2.1. General

This section elaborates the representative design methods in the literature and the proposed design methods in this study for chord sidewall failure in RHS joints. The bearing-buckling model proposed by Wardenier and Davies [5] is widely adopted by international design codes, e.g., EN 1993-1-8 [7] and ISO 14346 [8], and design guides such as the CIDECT design guide No. 3 [9-10] and the IIW recommendations [11-13]. The design rules specified in these design codes and design guides are nearly the same for chord sidewall failure in mild steel RHS joints. Kuhn et al. [21] and Wardenier [22], among others, proposed modifications to the codified design method in order to reduce the conservatism and scatter of the resistance predictions. Other analytical models were also proposed for chord sidewall failure, e.g., the four-hinge yield line model in combination with a reduced chord sidewall buckling length proposed by Yu [19], and the plate buckling models proposed by Becque and Cheng [20] and Lan et al. [23-24]. Two alternative design methods, i.e., a modified bearing-buckling method and a so-called “Lan-Kuhn method” are proposed herein. These design proposals are summarised in the subsequent sections. It is noted that steel with a grade up to S355 is defined as mild steel in this study.

2.2. Codified bearing-buckling model

Fig. 2 shows the codified bearing-buckling model for chord sidewall failure in RHS joints under brace axial loading [7, 8, 25]. It is based on a combined check for the bearing resistance using the steel yield stress of the chord (f_{y0}) and the local buckling capacity employing the local buckling stress of the chord sidewall (f_k). The f_k values can be obtained using the relevant Eurocode buckling curves [6] or equivalent buckling curves. Chord sidewall failure is conservatively considered as the buckling of a pinned-end strut with a buckling length of h_0-2t_0. The spreading of the normal component of the brace load ($N_1\sin\theta_1$) is assumed to be over a length of $h_1/\sin\theta_1+5t_0$ at each chord sidewall with a dispersion slope of 2.5 to 1 through the chord thickness. This results in the following basic resistance equation for chord sidewall failure in mild steel RHS joints under brace axial loading:

$$N_{1,\mathrm{Rd}} = \frac{f_k t_0}{\sin\theta_1}\left(\frac{2h_1}{\sin\theta_1}+10t_0\right)Q_f \tag{1}$$

where t_0 is the chord sidewall thickness, h_1 is the brace height, θ_1 is the brace angle (see Fig. 2) and Q_f is a chord stress function which accounts for the effect of longitudinal chord stresses. The term f_k, which equals f_{y0} for brace axial tension, is the buckling stress of the chord sidewall for brace axial compression, and is taken as [7, 8, 25]:

$$f_k = \begin{cases} 0.8\chi_C f_{y0} \sin\theta_1 & \text{for X joints} \\ \chi_C f_{y0} & \text{for T and Y joints} \end{cases} \quad (2)$$

where χ_C is a buckling reduction factor for column buckling according to EN 1993-1-1 [6], or a comparable design code, for a normalized slenderness (λ_C) defined by [7, 8, 25]:

$$\lambda_C = \frac{3.46\left(\frac{h_0}{t_0} - 2\right)\sqrt{\frac{1}{\sin\theta_1}}}{\pi\sqrt{\frac{E}{f_{y0}}}} \quad (3)$$

The Eurocode buckling reduction factor (χ_C) can be obtained from tables as a function of the normalized slenderness or by substituting Eq. (3) into Eqs. (4-5) where α is an imperfection factor. For cold-formed steel cross-sections, a buckling curve c with α=0.49 is used, and a buckling curve a with α=0.21 is adopted for hot-finished steel cross-sections using steel grades up to S420.

$$\chi = \frac{1}{\varphi + \sqrt{\varphi^2 - \lambda^2}} \leq 1.0 \quad (4)$$

$$\varphi = 0.5\left(1 + \alpha\left(\lambda - 0.2\right) + \lambda^2\right) \quad (5)$$

It is noted that the f_k value is reduced by including $\sin\theta_1$ in the f_k function for X joints (see Eq. (2)) and by incorporating the term of $(1/\sin\theta_1)^{0.5}$ in the λ_C equation (see Eq. (3)). This is because the research conducted by Platt [18] showed that the effect of θ_1 on the resistance of a chord sidewall, in an RHS X joint with θ_1<90°, is considerably smaller than being proportional to $1/\sin\theta_1$. Furthermore, a reduction factor of 0.8 (see Eq. (2)) (i.e., a safety factor of 1.25) was adopted for RHS X joints to increase the safety margin for the X joints with higher chord sidewall slenderness (h_0/t_0) which exhibit less-ductile failure.

Initially, no chord stress function (Q_f) was included for chord sidewall failure because the influence of small chord stresses is insignificant. Later on, based on the research by Wardenier et al. [26], the following Q_f functions, which are the same for β=1.0, were adopted for RHS T, Y and X joints [8, 25]:

$$Q_f = (1 - |n|)^{0.6-0.5\beta} \quad \text{for chord compression stress } (n<0) \quad (6)$$

$$Q_f = (1 - |n|)^{0.1} \quad \text{for chord tension stress } (n\geq 0) \quad (7)$$

where n is the normal (longitudinal) stress ratio in the chord connecting face. The n value is taken as the sum of the ratio of the chord axial force ($N_{0,Ed}$) to the chord axial yield capacity ($N_{pl,0,Rd}$) and the ratio of the chord bending moment ($M_{0,Ed}$) to the chord plastic moment capacity ($M_{pl,0,Rd}$). Negative and positive n values denote chord compression and tension stresses, respectively.

The resistance equations for chord sidewall failure in mild steel RHS X, T and Y joints under brace axial loading have been extended for brace in-plane bending (see Eq. (8)) and for brace out-of-plane bending (see Eq. (9)) as follows [8, 10, 25]:

$$M_{ip,1,Rd} = 0.5\chi_C f_{y0} t_0 \left(h_1 + 5t_0\right)^2 Q_f \quad (8)$$

$$M_{\mathrm{op,1,Rd}} = \chi_{\mathrm{C}} f_{\mathrm{y0}} t_0 \left(b_0 - t_0\right)\left(h_1 + 5t_0\right) Q_{\mathrm{f}} \tag{9}$$

which are conservative for θ_1<90°. For brace out-of-plane bending, it is presumed that the chord distortion failure mode is prevented.

The aforementioned developments resulted in the resistance equations summarized in Table 1, which have been adopted by recent international design codes and design guides [8, 10, 13, 25]. Up to 2013, the design recommendations applied to a nominal yield stress (f_{y0}) of the finished hollow section up to 460 MPa, with the f_{y0} value for design not exceeding 0.8 times the ultimate stress of the chord (f_{u0}). The stipulated joint resistances in the design recommendations [8, 10, 13] were to be multiplied by a material factor (C_f) of 0.90 for 355 MPa < f_{y0} ≤ 460 MPa. The most recent prEN 1993-1-8 [25] has proposed: C_f = 1.00 for f_{y0} ≤ 355 MPa, C_f = 0.90 for 355 MPa < f_{y0} ≤ 460 MPa, C_f = 0.86 for 460 MPa < f_{y0} ≤ 550 MPa, and C_f = 0.80 for 550 MPa < f_{y0} ≤ 700 MPa.

2.3. Modifications to codified bearing-buckling model

2.3.1. Linearized buckling reduction factor proposed by Kuhn et al. [21]

Kuhn et al. [21] showed that the column buckling reduction factor ($\chi_{0.5}$) for mild steel cold-formed RHS decreases in an approximately linear manner with increasing h_0/t_0 ratio up to 50. The $\chi_{0.5}$ value was obtained using a reduced chord sidewall slenderness ($\lambda_{0.5}$), which was first suggested by Yu [19]:

$$\lambda_{0.5} = 0.5\lambda_{\mathrm{C}} \tag{10}$$

It is assumed that the chord sidewall is fixed along the longitudinal edges, and thus the $\lambda_{0.5}$ value is taken as half of that adopted in Table 1. Kuhn et al. [21] proposed to express the buckling reduction factor as a linear function of the h_0/t_0 ratio and also to include empirical terms of $(1/\sin\theta_1)^{0.5}$ and $(f_{y0}/350)^{0.5}$ to consider the effects of brace angle and steel grade. These proposals resulted in the following linearized equation of the buckling reduction factor for RHS X joints having $h_1/(h_0\sin\theta_1)$ > 0.25 [21]:

$$\chi_{\mathrm{Kuhn}} = 1.15 - 0.013\frac{h_0}{t_0}\sqrt{\frac{1}{\sin\theta_1}}\sqrt{\frac{f_{\mathrm{y0}}}{350}} \le 1.0 \tag{11}$$

For plate-to-RHS X joints and RHS-to-RHS X joints with $h_1/(h_0\sin\theta_1)\le 0.25$, $\chi_{\mathrm{Kuhn}}=1.0$ is proposed to be used within the general validity range given in Table 1, and the resistance for chord sidewall failure in RHS X joints under brace axial compression can be obtained from [21]:

$$N_{\mathrm{Kuhn}} = \chi_{\mathrm{Kuhn}} f_{\mathrm{y0}} t_0 \left(\frac{2h_1}{\sin\theta_1} + 10t_0\right) Q_{\mathrm{f}} \tag{12}$$

It is noted that the term of $f_k t_0/\sin\theta_1$ in Eq. (1) becomes $\chi f_{y0} t_0$ when substituting $f_k=\chi f_{y0}\sin\theta_1$ for RHS X joints.

The moment capacities for chord sidewall failure in RHS X joints under brace in-plane bending ($M_{\mathrm{ip,Kuhn}}$) and brace out-of-plane bending ($M_{\mathrm{op,Kuhn}}$) may be obtained from Eqs. (8-9), but replacing χ_{C} with χ_{Kuhn} in Eq. (11).

2.3.2. η correction proposed by Wardenier [22]*

Apart from using the reduced chord sidewall slenderness ($\lambda_{0.5}$) for RHS joints that are sufficiently restrained against out-of-plane movements, Wardenier [22] proposed to reconsider the effect of brace-to-chord height ratio (η*=h_1/h_0). This is because the numerical results of Yu [19] and Lan et al. [23-24] show that full-width RHS X and T joints with higher η* and 2γ* (=h_0/t_0) ratios have a more-abrupt chord sidewall failure mode, i.e., the load-deformation curve exhibits a sharp drop in load after the peak load. Thus, it would be logical to increase at least the safety margin for RHS joints with a less-ductile failure mode.

Wardenier [22] proposed to include a correction function of $(h_1/h_0)^{-0.15}$ in the resistance equation (see Eq. (1)) in order to increase the safety margin for full-width RHS joints with a less-ductile failure mode. The modified resistance equations for RHS X joints with θ_1=90° and under brace axial compression then become:

$$N_{\text{Ward}} = f_{\text{k,Ward}} t_0 \left(2h_1 + 10t_0\right)\left(\frac{h_0}{h_1}\right)^{0.15} Q_{\text{f}} \tag{13}$$

$$f_{\text{k,Ward}} = \chi_{\text{Ward}} f_{\text{y0}} \tag{14}$$

where χ_{Ward} is the buckling reduction factor obtained using the Eurocode buckling curve c and the chord sidewall slenderness ($\lambda_{0.5}$) or the linearized approximation, e.g., as proposed by Kuhn et al. [21] (see Eq. (11)). Using Eq. (13) would result in an equal or higher safety margin for the less-ductile RHS joints when compared with the more-ductile joints with low η* and 2γ* ratios.

The moment capacities for chord sidewall failure in RHS X joints under brace in-plane bending and brace out-of-plane bending may be obtained using Eqs. (8-9), but replacing χ_{C} with χ_{Ward}. It is also worth noting that the initial analyses conducted by Wardenier [22] indicate that the brace angle effect needs to be reconsidered.

2.4. Representative analytical models

2.4.1. Four-hinge yield line model proposed by Yu [19]

In the 1990s, Yu [19] conducted an extensive study on uniplanar and multiplanar RHS joints. A four-hinge yield line model (see Fig. 3) was proposed for chord sidewall failure in RHS-to-RHS X and T joints under brace axial compression, brace in-plane bending and brace out-of-plane bending. The corresponding resistance equation for mild steel RHS-to-RHS X and T joints, with θ_1=90° and under brace axial compression, is as follows:

$$N_{\text{Yu}} = 4\chi_{0.5}\left(\sqrt{\gamma} + \gamma\eta\right) f_{\text{y0}}\, t_0^2 \tag{15}$$

where γ (=$b_0/2t_0$) is the chord width to twice chord wall thickness ratio, η (=h_1/b_0) is the brace height to chord width ratio, and $\chi_{0.5}$ is the buckling reduction factor determined by substituting $\lambda_{0.5}$ (see Eq. (10)) into Eqs. (4-5). The four-hinge yield line model assumes that the chord sidewalls are fixed along the longitudinal edges.

The moment capacity of chord sidewall failure in mild steel RHS-to-RHS T and X joints, with θ_1=90° and loaded under brace in-plane bending, is given by:

$$M_{\mathrm{ip,Yu}} = \chi_{\mathrm{ip,0.5}} \left(2\sqrt{\gamma} + \gamma\eta + \frac{1}{2\eta} \right) f_{y0} t_0^2 h_1 \tag{16}$$

where $\chi_{\mathrm{ip,0.5}}$ is the buckling reduction factor which equals 1.0 for $\eta \leq 1$ and for $1 < \eta \leq 2$, is determined by:

$$\chi_{\mathrm{ip,0.5}} = 1 + (\eta - 1) \left(\frac{1}{\varphi + \sqrt{\varphi^2 - \lambda_{0.5}{}^2}} - 1 \right) \tag{17}$$

The moment capacity of chord sidewall failure in mild steel RHS-to-RHS T and X joints, with θ_1=90° and loaded under brace out-of-plane bending, is given by:

$$M_{\mathrm{op,Yu}} = \chi_{0.5} \left(\sqrt{2(1+2\gamma)} + 2\gamma\eta \right) f_{y0} t_0^2 b_1 \tag{18}$$

2.4.2. Plate buckling model proposed by Becque and Cheng [20]

Becque and Cheng [20] proposed a plate buckling model conservatively assuming that the chord sidewall is pinned along the longitudinal edges for chord sidewall failure in RHS-to-RHS X joints under brace axial compression. The corresponding resistance equation is as follows:

$$N_{\mathrm{Becque}} = 2.4 \chi_{\mathrm{Becque}} f_{y0} h_1 t_0 \tag{19}$$

where χ_{Becque} is the buckling reduction factor obtained using the relevant buckling curve, e.g., according to Eqs. (4-5); however, a modified imperfection factor α=0.08 is recommended and the proposed chord sidewall slenderness is as follows:

$$\lambda_{\mathrm{Becque}} = \sqrt{\frac{P_y}{P_{cr}}} = \sqrt{\frac{2.4 f_{y0} h_1 t_0}{2 f_{\mathrm{cr,Becque}} h_1 t_0}} \tag{20}$$

$$f_{\mathrm{cr,Becque}} = 1.346 \frac{\pi^2 E}{12(1-\nu^2)} \frac{t_0^2}{h_0 h_1} \tag{21}$$

where E is the steel elastic modulus and ν is the Poisson ratio taken as 0.3.

It is noted that this design method is proposed to predict the initiation of buckling of the chord sidewall. This buckling load can be considerably lower than the joint resistance determined by the peak load or the load at an indentation limit of 3%b_0, whichever occurs at a smaller deformation, which is commonly adopted in other studies. This design method is therefore not included in the subsequent evaluation.

2.4.3. Plate buckling model proposed by Lan et al. [23-24]

The restraint from the chord face and the brace to the chord sidewall is stronger than that of a pinned-end boundary condition, but weaker than that of fixed edges. Lan et al. [23] proposed an analytical model of plate buckling for chord sidewall failure in RHS-to-RHS X joints which can properly consider the restraint and utilize the strain hardening of steel materials by using the continuous strength method. Later, Lan et al. [24] simplified the resistance equations without considering the strain hardening for RHS-to-RHS X and T joints to reduce the computational effort. It is noted that the strain hardening in high-strength steel is not pronounced. Fig. 4 shows the proposed plate buckling model for RHS-to-RHS X and T joints with θ_1=90°.

The elastic buckling stress equation proposed for RHS-to-RHS T and X joints with θ_1=90°, which can properly consider the restraint from the chord face and the brace to the chord sidewall, is as follows [23-24]:

$$f_{\mathrm{cr,Lan}} = 3.2\frac{\pi^2 E}{12(1-\nu^2)}\left(\frac{t_0}{h_0}\right)^{1.96}\left(\frac{h_0}{h_1}\right)^{0.66} \qquad (22)$$

The overall cross-section slenderness of the chord sidewall is defined by [23-24]:

$$\lambda_{\mathrm{Lan}} = \sqrt{\frac{f_{\mathrm{y0}}}{f_{\mathrm{cr,Lan}}}} \qquad (23)$$

which can be obtained by substituting Eq. (22), E=210000 MPa and ν=0.3 into Eq. (23):

$$\lambda_{\mathrm{Lan}} = 0.024\left(\frac{h_0}{t_0}\right)^{0.98}\left(\frac{h_1}{h_0}\right)^{0.33}\sqrt{\frac{f_{\mathrm{y0}}}{355}} \qquad (24)$$

which can be conservatively approximated by rounding off the exponents:

$$\lambda_{\mathrm{Lan}} = 0.024\frac{h_0}{t_0}\left(\frac{h_1}{h_0}\right)^{0.3}\sqrt{\frac{f_{\mathrm{y0}}}{355}} \qquad (25)$$

The plate buckling reduction factor (χ_{Lan}) neglecting the strain hardening, which is based on the base curves proposed by Lan et al. [23], is as follows [24]:

$$\chi_{\mathrm{Lan}} = \begin{cases} 1.0 & \text{for } \lambda_{\mathrm{Lan}} \le 0.6 \\ 0.8\left(1-\dfrac{0.2}{\lambda_{\mathrm{Lan}}^{1.6}}\right)\dfrac{1}{\lambda_{\mathrm{Lan}}^{1.6}} & \text{for } \lambda_{\mathrm{Lan}} > 0.6 \end{cases} \qquad (26)$$

The curve of the χ_{Lan} equation is relatively linear for χ_{Lan}>0.6 and is herein suggested to be approximated by:

$$\chi_{\mathrm{Lan}} = 1.39 - 0.67\lambda_{\mathrm{Lan}} \le 1.0 \qquad (27)$$

which can be obtained by substituting Eq. (25) into Eq. (27) for steel grades up to S960 and ratios of b_0/t_0 and h_0/t_0 up to 40:

$$\chi_{\mathrm{Lan}} = 1.39 - 0.016\frac{h_0}{t_0}\left(\frac{h_1}{h_0}\right)^{0.3}\sqrt{\frac{f_{\mathrm{y0}}}{355}} \le 1.0 \qquad (28)$$

The linearized buckling reduction factor (see Eq. (28)) can produce conservative resistance prediction for RHS joints using higher steel grades in combination with ratios of b_0/t_0 and h_0/t_0 larger than 35, and thus the original Eqs. (25-26) are suggested for such cases.

The joint resistance (N_{Lan}) for chord sidewall failure in RHS-to-RHS T and X joints with θ_1=90° can be obtained from [24]:

$$N_{\mathrm{Lan}} = \chi_{\mathrm{Lan}} f_{\mathrm{y0}} t_0 \left(2h_1 + 10t_0\right) Q_{\mathrm{f}} \qquad (29)$$

The joint resistance for chord sidewall failure in RHS-to-RHS T, Y and X joints under brace in-plane bending and brace out-of-plane bending may be obtained from Eqs. (8-9), but replacing χ_{C} with χ_{Lan} in Eq. (28). The linearized Lan method using Eqs. (28-29) will be examined in the subsequent analyses.

2.5. Proposed design methods

2.5.1. General

Lan et al. [23-24, 27-28] evaluated the material effect on the resistance of fabricated RHS and CHS X and T joints under brace axial compression and proposed the following equation for the material factor (C_f) to quantify the resistance reduction, which was resulted from the material effect:

$$C_f = 1.1 - 62\, f_{y0}/E \le 1.0 \tag{30}$$

An equivalent C_f equation as a function of only f_{y0} is proposed in this study to maintain a uniform format for equations:

$$C_f = 1.1 - 0.1\, f_{y0}/355 \le 1.0 \tag{31}$$

The differences between the calculated C_f values using Eqs. (30-31) are found to be marginal. The derived C_f values are 1.00, 0.97, 0.90, 0.85 and 0.83 for steel grades of S355, S460, S700, S900 and S960, respectively. The corresponding rounded-off C_f values of 1.00, 0.95, 0.90, 0.85 and 0.80 may be used for chord sidewall failure under brace compression loading, which are more optimistic than the general C_f values stipulated in prEN 1993-1-8 [25]. Eq. (31) is incorporated in the proposed design methods mainly because significant material softening in the heat-affected zone of high-strength steel can occur in practice and the effect of fabrication imperfections can be more pronounced for chord sidewall failure in high-strength steel RHS joints (see Section 5).

The codified bearing-buckling method adopts various compensations for the brace angle effect in RHS X joints by including $\sin\theta_1$ in f_k and $(1/\sin\theta_1)^{0.5}$ in λ_C (see Section 2.2). It is noted that the correction of $\sin\theta_1$ and safety factor of 0.8 in f_k are not adopted for RHS T and Y joints (see Eq. (2)). This leads to inconsistences for the design of RHS X and T/Y joints. The brace angle effect for RHS X, T and Y joints is herein recommended to be approximated by only using a function of $(1/\sin\theta_1)^{0.5}$ in the final resistance equation, which is in line with Davies and Roodbaraky [17].

Wardenier [22] proposed to adopt a correction function of $(h_1/h_0)^{-0.15}$ for the design joint resistance (see Eq. (13)). However, it is more suitable, e.g., for the loading case of brace axial tension, to include the term of $(h_1/h_0)^{-0.15}$ in the f_k function and to impose an upper limit of f_{y0} for f_k values, and thus the design joint resistance can be limited by the yield resistance.

The aforementioned proposed modifications result in the basic resistance equation for chord sidewall failure in RHS X, T and Y joints under brace axial compression as follows:

$$N_P = C_f\, f_{k,P} t_0 \left(2h_1 + 10t_0\right) \sqrt{\frac{1}{\sin\theta_1}} Q_f \tag{32}$$

$$f_{k,P} = \chi_P \left(\frac{h_0}{h_1}\right)^{0.15} f_{y0} \le f_{y0} \tag{33}$$

where C_f is the proposed material factor (see Eq. (31)), $t_0(2h_1+10t_0)$ is the bearing area taken in line with the bearing-buckling model, Q_f is the chord stress function (see Eqs. (6-7)), $(1/\sin\theta_1)^{0.5}$ is the brace angle function, $f_{k,P}$ is the buckling stress of the chord sidewall and χ_P is the proposed buckling reduction factor. Two alternative methods are proposed to derive the χ_P values in this study.

2.5.2. Modified bearing-buckling method

Some code committees prefer, as currently used, a design method for chord sidewall failure which adopts the column buckling curve, in order to maintain consistency between the design of RHS joints and that of members. A format similar to the current set-up in the design codes and design guides was thus employed. The proposed modified bearing-buckling method in this study adopts a buckling curve c with α=0.49 in EN 1993-1-1 [6] and a reduced chord sidewall slenderness of $\lambda_{0.5}$ (see Eq. (10)). The buckling reduction factor ($\chi_{P,M}$) can therefore be obtained from:

$$\chi_{P,M} = \frac{1}{\varphi_M + \sqrt{\varphi_M^2 - \lambda_{0.5}^2}} \leq 1.0 \tag{34}$$

$$\varphi_M = 0.5\left(1 + 0.49\left(\lambda_{0.5} - 0.2\right) + \lambda_{0.5}^2\right) \tag{35}$$

where $\chi_{P,M}$ is the proposed modified buckling reduction factor. It is noted that the codified bearing-buckling method and the four-hinge yield line model adopt different buckling curves according to the fabrication methods of cross-sections (e.g., cold-formed or hot-finished). However, a buckling curve c is herein suggested for all cross-sections to simplify the design process and to produce resistance predictions on the conservative side.

2.5.3. Lan-Kuhn method

The linearized Kuhn method is based on the combined bearing-buckling model with the chord sidewall assumed to be fixed along the longitudinal edges and local buckling covered by the strut buckling coefficient [5,29], whereas the linearized Lan method is based on a plate local buckling model. In reality, bearing governs for low h_0/t_0 ratios and local buckling dominates for higher h_0/t_0 ratios. Therefore, the Lan-Kuhn method using a linearized function of buckling reduction factor is proposed in this study.

The effect of h_1/h_0 ratio is not considered in the Kuhn method. The Lan method adopts a term of $(h_1/h_0)^{0.3}$ in the buckling reduction factor (see Eq. (28)) to quantify the effect, and this approach was initially considered for the Lan-Kuhn method. However, it was found that this could result in large deviations of the predicted resistances especially for $\eta^*\neq1.0$ when compared with the proposed modified bearing-buckling method. It is noted that two alternative design methods should give comparable resistances. More detailed discussions can be found in Wardenier et al. [30]. Therefore, the influence of h_1/h_0 ratio is included in the buckling stress equation (see Eq. (33)), and the effect of θ_1 is considered in the basic resistance equation (see Eq. (32)) in this study. Only the effects of the h_0/t_0 ratio and f_{y0} are quantified in the proposed equation for the buckling reduction factor ($\chi_{P,LK}$):

$$\chi_{P,LK} = 1.12 - 0.012\frac{h_0}{t_0}\sqrt{\frac{f_{y0}}{355}} \leq 1.0 \tag{36}$$

The joint resistance for chord sidewall failure in RHS X, T and Y joints under brace in-plane bending and brace out-of-plane bending may be obtained from Eqs. (8-9), but replacing $\chi_C f_{y0}$ with $f_{k,P}$ in Eq. (33).

2.5.4. Comparison of the buckling reduction factors

Table 2 shows a comparison of $\chi_{P,LK}$, χ_{Kuhn} and χ_{Lan} with $\chi_{P,M}$ for $h_0/t_0 \leq 40$, $h_1/h_0=1.0$, 235 MPa $\leq f_{y0} \leq$ 960 MPa and $\theta_1=90°$. The $\chi_{P,LK}/\chi_{P,M}$, $\chi_{Kuhn}/\chi_{P,M}$, and $\chi_{Lan}/\chi_{P,M}$ ratios equal the corresponding resistance ratios because $h_1/h_0=1.0$ and the same basic resistance equation (Eq. (1)) is adopted. It is shown that the differences between $\chi_{P,LK}$ and $\chi_{P,M}$ are minor with a maximum deviation of 4%. These two proposed design methods therefore give almost equivalent resistances. The χ_{Kuhn} equation also produces excellent approximations of $\chi_{P,M}$ values for lower steel grades; however, it is observed that the χ_{Kuhn} value deviates from the $\chi_{P,M}$ value for steel grades of S700 and higher in combination with a high h_0/t_0 ratio. The maximum deviation is 4% for steel grades up to S700 and becomes 16% for S960 which is on the conservative side. It is also shown that χ_{Lan} values are generally higher than $\chi_{P,M}$ values with a maximum discrepancy of 20% because the Lan method is based on a plate buckling model and is not related to the column buckling curves. It should be noted that the deviations of χ_{Kuhn} and χ_{Lan} values from $\chi_{P,M}$ values could be larger for $h_1/h_0<1.0$ and $h_1/h_0>1.0$ because the effect of the h_1/h_0 ratio is not considered in χ_{Kuhn} for the Kuhn method; however, it is considered in χ_{Lan} for the Lan method and in $f_{k,P}$ for the proposed modified bearing-buckling method. More detailed information can be found in Wardenier et al. [30].

3. Evaluation of design methods for full-width RHS X and T joints under brace axial compression

3.1. General

A database of test and numerical results totalling 248 full-width RHS X joints under brace axial compression reported in the literature was established. Results of plate-to-RHS X joints were analysed by Kuhn et al. [21] and are not further considered in this study. The compiled results were adopted to evaluate the following six design methods:

(1) The bearing-buckling method, but using the Eurocode buckling curve c and $\lambda_{0.5}$ with $N_{C,M}$ defined by Eqs. (1) and (10)

(2) The Kuhn linearized method in Section 2.3.1 with N_{Kuhn} defined by Eqs. (11-12)

(3) The Yu four-hinge yield line method in Section 2.4.1 with N_{Yu} defined by Eqs. (10) and (15)

(4) The Lan plate buckling method using the linearized approach in Section 2.4.3 with N_{Lan} defined by Eqs. (28-29)

(5) The bearing-buckling method, but using the Eurocode buckling curve c, $\lambda_{0.5}$ and $(\eta^*)^{-0.15}$ correction in Section 2.5.2 with $N_{P,M}$ defined by Eqs. (32-35)

(6) The Lan-Kuhn method using the linearized approach in Section 2.5.3 with $N_{P,LK}$ defined by Eqs. (32-33) and (36)

The original equations in Section 2 are used in this study unless specified. The corresponding joint resistances obtained using the six design methods ($N_{C,M}$, N_{Kuhn}, N_{Yu}, N_{Lan}, $N_{P,M}$ and $N_{P,LK}$) will be compared with the test and numerical resistances (N_{1u}) in the subsequent sections. It should be noted that $N_{C,M}$=$N_{P,M}$ for η*=1.0, and the effect of the η* correction could be evaluated by comparing $N_{C,M}$ with $N_{P,M}$ for η*<1 and η*>1.

It should be noted that the safety factor of 1.25 for RHS X joints, adopted by the aforementioned design codes and design guides, was set to be unity in the assessment of the design methods. The Eurocode buckling curve c was conservatively used for all RHS joints, regardless of whether tests or numerical models used hot-finished or cold-formed hollow sections. In addition, RHS joints with N_{1u}/N_y>1.1, where N_y is the joint yield resistance, were excluded from the analyses because such data may not be realistic and could lead to a large scatter for the subsequent statistical analyses. The N_y values for all the design methods in this study is obtained from:

$$N_y = f_{y0} t_0 \left(2h_1 + 10t_0\right)\sqrt{\frac{1}{\sin\theta_1}} \quad (37)$$

where the term $(1/\sin\theta_1)^{0.5}$ is adopted to consider the brace angle effect, in line with Davies and Roodbaraky [17], and the Q_f function is not incorporated. For this comparison, the omission of Q_f function is conservative, especially for large absolute values of chord stress ratio (n), as it leads to lower N_{1u}/N_y ratios.

3.2. Test results of RHS-to-RHS X joints

Table 3 summarises the compiled test results totalling 51 full-width RHS-to-RHS X-joints under brace axial compression. Source references for most tests are given in Kuhn et al. [21] and Fan [31]. Additional test results of high-strength steel RHS-to-RHS X joints reported by Feldmann et al. [32] and Pandey and Young [33] were also collated. It is shown that five RHS joints have resistances exceeding 1.1N_y and therefore only the remaining 46 RHS-to-RHS X joints will be included in the subsequent analyses. The parameter ranges for the screened test database were β=1.0, 12.6≤2γ≤42.2, 12.6≤2γ*≤56.9, 0.50≤η≤2.47, 0.60≤η*≤1.00, -0.87≤n≤0, 44°≤θ_1≤90° and 228 MPa≤f_{y0}≤1080 MPa. Cold-formed and hot-finished RHS were covered.

The brace angle effect is re-evaluated against the test results of RHS-to-RHS X joints with varying brace angles in this study. Davies et al. [14] and Packer [15] found that the effect of brace angle on the resistance of full-width RHS X joints is smaller than being proportional to $1/\sin\theta_1$. Davies and Roodbaraky [17] reported that, for brace axial compression and tension, the enhancement of resistance for decreasing the brace angle could be more accurately quantified by a function of $(1/\sin\theta_1)^{0.5}$. Therefore, in the current codified design rules (see Table 1), the brace angle effect is, based on the initial investigations by Platt [18], minimised by various compensations in the chord sidewall slenderness (λ_C) and the buckling stress (f_k) for the X joints. It is noted that the term of $f_k t_0/\sin\theta_1$ in Eq. (1) becomes $\chi f_{y0} t_0$ when substituting $f_k=\chi f_{y0}\sin\theta_1$ for RHS X joints. The following two options are assessed against test results of 19 selected RHS-to-RHS X joints with θ_1≤90°:

(1) Using the codified term of $h_1/\sin\theta_1$ in the final resistance equation for $N_{C,M}$, N_{Kuhn}, N_{Lan}, $N_{P,M}$ and $N_{P,LK}$, and also including a term of $(1/\sin\theta_1)^{0.5}$ in $\lambda_{0.5}$ for $N_{C,M}$ and $N_{P,M}$ and in χ_{Kuhn} for N_{Kuhn} (see Table 4). Including a $1/\sin\theta_1$ term in the final resistance equation for N_{Yu}.

(2) Only incorporating a term of $(1/\sin\theta_1)^{0.5}$ in the final resistance equation for $N_{C,M}$, N_{Kuhn}, N_{Yu}, N_{Lan}, $N_{P,M}$, and $N_{P,LK}$ (see Table 5).

The material factor (C_f) was not used for all the statistical analyses summarised in Tables 4-5 because the variation in yield stresses is small. The mean values of $N_{1u}/N_{C,M}$, N_{1u}/N_{Yu}, N_{1u}/N_{Kuhn}, N_{1u}/N_{Lan}, $N_{1u}/N_{P,M}$ and $N_{1u}/N_{P,LK}$ ratios are 1.11, 1.02, 1.13, 0.89, 1.11 and 1.05, respectively, with corresponding coefficients of variation (CoVs) of 0.103, 0.103, 0.105, 0.101, 0.103 and 0.104 for the first approach (Table 4). However, for the second option, the mean values of $N_{1u}/N_{C,M}$, N_{1u}/N_{Yu}, N_{1u}/N_{Kuhn}, N_{1u}/N_{Lan}, $N_{1u}/N_{P,M}$ and $N_{1u}/N_{P,LK}$ ratios are 1.12, 1.05, 1.13, 0.95, 1.12 and 1.12, respectively, with corresponding CoVs of 0.086, 0.079, 0.087, 0.082, 0.086 and 0.085 (Table 5). It is shown that the CoV values of the various design methods for each option are close. The mean values for the second option are slightly higher and the corresponding CoV values are about 20% lower when compared with those employing the first solution. Therefore, only including a term of $(1/\sin\theta_1)^{0.5}$ in the final resistance equation, which is simpler and yields more consistent resistance predictions, is recommended to account for the brace angle effect.

The chord stress effect was assessed against test results of eight available RHS-to-RHS X joints with θ_1=90° and varying chord stress ratios (n) summarised in Table 6. The codified Q_f function was adopted for all the design methods in the statistical analyses and C_f =1.0 was used for all the mild steel X joints. The mean values of $N_{1u}/N_{C,M}$, N_{1u}/N_{Yu}, N_{1u}/N_{Kuhn}, N_{1u}/N_{Lan}, $N_{1u}/N_{P,M}$ and $N_{1u}/N_{P,LK}$ ratios are 1.21, 1.13, 1.22, 1.03, 1.21 and 1.23, respectively, with corresponding CoVs of 0.088, 0.088, 0.088, 0.089, 0.088 and 0.088. All the design methods yield almost the same CoVs because only the chord stress ratio is different for each test series and all other parameters are nearly the same. It is also observed that the resistance ratios, which generally exceed 1.0, increase with increasing absolute value of n ratio because for high $|n|$ values the Q_f function adopts a conservative lower bound for the chord stress effect.

The material effect was evaluated against the screened database of 46 RHS-to-RHS X joints in Tables 7-8. The approach of only including a term of $(1/\sin\theta_1)^{0.5}$ in the final resistance equation was adopted for all design methods to reveal the best performance of these methods. For the design methods without using the proposed C_f factor (see Table 7), the mean values of $N_{1u}/N_{C,M}$, N_{1u}/N_{Yu}, N_{1u}/N_{Kuhn}, N_{1u}/N_{Lan}, $N_{1u}/N_{P,M}$ and $N_{1u}/N_{P,LK}$ ratios are 1.13, 1.05, 1.15, 0.97, 1.12 and 1.13, respectively, with corresponding CoVs of 0.098, 0.096, 0.098, 0.097, 0.097 and 0.097. For the design methods using the C_f factor (see Table 8), the mean values of $N_{1u}/N_{C,M}$, N_{1u}/N_{Yu}, N_{1u}/N_{Kuhn}, N_{1u}/N_{Lan}, $N_{1u}/N_{P,M}$ and $N_{1u}/N_{P,LK}$ ratios are 1.17, 1.10, 1.20, 1.01, 1.17 and 1.17, respectively, with corresponding CoVs of 0.092, 0.086, 0.116, 0.116, 0.091 and 0.095. Thus, including the C_f factor reduces the CoVs except for the Kuhn method and the Lan method, which both use the linearized approach. This is mainly because the Kuhn and Lan methods are conservative for the S960 specimens tested by Pandey and Young [33].

The design methods without using the C_f factor often yield unconservative resistance predictions for the test specimens with yield stresses higher than 900 MPa (see Table 7). In contrast, including the C_f factor in the design methods leads to safe resistance predictions for all the high-strength steel test specimens (see Table 8). Thus, the proposed C_f factor is suggested to consider the material effect. It is also shown that the Yu method and the proposed modified bearing-buckling method give the lowest CoVs, and other design methods yield slightly higher CoVs. It should be noted that the low resistance ratios of the X5-S960 specimen (see Table 7) may be attributed to the material softening in the heat-affected zones and/or an insufficient weld size, as commented by Feldmann et al.

[32]. The test evidence for high-strength steel RHS joints remains limited, and more related test and numerical investigations are needed to assess the material effect comprehensively.

Most of the RHS-to-RHS X joints in Tables 7-8 have $\eta^*\approx1.0$ and there are only two X joints with small η^* values of 0.60 and 0.75. Thus, the effect of including the η^* correction in the f_k function cannot be fully revealed in the overall statistical analyses and has been checked in Section 3.3 using the numerical data.

3.3. Numerical results of RHS-to-RHS X joints

Table 9 summarises the collated numerical results totalling 173 RHS-to-RHS X joints with θ_1=90° reported by Yu [19] and Kuhn et al. [21]. It is shown that 42 RHS joints have resistances exceeding $1.1N_y$ and therefore only the remaining 131 joints will be used in the analyses. The parameter ranges for the screened numerical database were β=1.0, $10\leq2\gamma\leq35$, $10\leq2\gamma^*\leq35$, $0.25\leq\eta\leq2.00$, $0.21\leq\eta^*\leq2.50$, $-0.80\leq n\leq0.75$, θ_1=90° and f_{y0}=355 and 398 MPa. Cold-formed and hot-finished RHS are included. It is noted that all the RHS-to-RHS X joints had θ_1=90° and thus the brace angle effect cannot be evaluated. The C_f values for f_{y0}=355 and 398 MPa are 1.00 and 0.99, respectively, thus the material effect is insignificant for these X joints. Nevertheless, the C_f factor was adopted for all the design methods to allow for direct comparison.

The effect of the η^* ratio was examined against the numerical results of 22 selected RHS-to-RHS X joints with n=0 and $0.42\leq\eta^*\leq2.50$ (see Table 10). The mean values of $N_{1u}/N_{C,M}$, N_{1u}/N_{Yu}, N_{1u}/N_{Kuhn}, N_{1u}/N_{Lan}, $N_{1u}/N_{P,M}$ and $N_{1u}/N_{P,LK}$ ratios are 1.19, 1.11, 1.20, 1.05, 1.20 and 1.20, respectively, with corresponding CoVs of 0.105, 0.080, 0.106, 0.051, 0.064 and 0.059. It is shown that including the term of $(\eta^*)^{-0.15}$ in the $f_{k,P}$ (see Eq. (33)) of proposed design methods can reduce the CoV by about 40% when compared with the bearing-buckling method ($N_{C,M}$) and the Kuhn method (N_{Kuhn}) in which the η^* effect is not considered. Incorporating the term of $(\eta^*)^{0.3}$ in the buckling reduction factor (see Eq. (28)) of the Lan method can also significantly reduce the CoV and the improvement is slightly better than that of the proposed design methods. For the Lan-Kuhn model, including the $(\eta^*)^{0.3}$ term in $\chi_{P,LK}$ (see Eq. (36)), as used in the Lan method, instead of using the $(\eta^*)^{-0.15}$ correction in $f_{k,P}$ (see Eq. (33)), slightly increases the CoV for the joints in Table 10 from 0.059 to 0.062, and the deviations of $N_{P,LK}$ from $N_{P,M}$ become larger up to 7%. Thus, including the proposed η^* correction in $f_{k,P}$ is suggested.

The chord stress effect was assessed against numerical results of 10 selected RHS-to-RHS X joints with varying n ratios (see Table 11) reported by Yu [19]. The codified chord stress function (Q_f) was adopted for all the design methods in the statistical analyses. The mean values of $N_{1u}/N_{C,M}$, N_{1u}/N_{Yu}, N_{1u}/N_{Kuhn}, N_{1u}/N_{Lan}, $N_{1u}/N_{P,M}$ and $N_{1u}/N_{P,LK}$ ratios are 1.34, 1.25, 1.34, 1.15, 1.34 and 1.34, respectively, with corresponding CoVs of 0.074, 0.063, 0.073, 0.073, 0.074 and 0.064. The Yu and Lan-Kuhn methods yield the lowest CoVs and provide the most consistent strength predictions. It is also found that the resistance ratios, which all exceed 1.0, increase with increasing absolute values of the n ratio because the codified Q_f function employs a conservative lower bound for the chord stress effect. It is noted that these conclusions also apply to the numerical data with varying n ratios reported by Kuhn et al. [21] (see Table 12). Similar observations were reported by Kim et al. [34] for RHS X joints with β ratio up to 1.0 and with f_{y0}=324 MPa and 798 MPa, and also by Lan et al. [23] for fabricated RHS X joints with f_{y0}=460, 690 and 960 MPa. Thus, the need for new chord stress functions is not apparent, and Eqs. (6-7) can be adopted.

Table 12 shows the results of statistical analyses for the evaluation of all the design methods against the screened numerical database of 131 RHS-to-RHS X joints. The mean values of $N_{1u}/N_{C,M}$, N_{1u}/N_{Yu}, N_{1u}/N_{Kuhn}, N_{1u}/N_{Lan}, $N_{1u}/N_{P,M}$ and $N_{1u}/N_{P,LK}$ ratios are 1.24, 1.15, 1.25, 1.10, 1.23 and 1.24, respectively, with corresponding CoVs of 0.102, 0.082, 0.104, 0.061, 0.065 and 0.064. It is demonstrated that the Lan method and the proposed design methods produce the lowest CoVs and thus most consistent resistance predictions.

3.4. Summary for RHS-to-RHS X joints

The overall statistical analyses for the test database (see Tables 7-8) show that the Yu method gives the lowest CoVs; however, the differences with other design methods are small. The approach of only incorporating a term of $(1/\sin\theta_1)^{0.5}$ in the final resistance equation can more accurately quantify the brace angle effect and is preferred. Including the C_f factor reduces the CoVs for all the design methods except for the Kuhn method and the Lan method. Incorporating the C_f factor in all the design methods can yield safe resistance predictions for high-strength steel test specimens and is preferred; however, more experimental and numerical studies on high-strength steel joints are needed to further confirm the proposed C_f factor. The codified chord stress function (Q_f) is more conservative for larger absolute values of n ratio. It is noted that only two X joints had small η^* ratios in the test database, and thus the evaluation of η^* effect is based on the numerical data.

The overall statistical analyses for the numerical database (see Table 12) show that the Lan method and the proposed design methods (i.e., the proposed modified bearing-buckling method and the Lan-Kuhn method) produce the lowest CoVs. It is demonstrated that the effect of the η^* ratio on the joint resistance is significant. Including the η^* correction in the buckling reduction factor or the buckling stress equation results in more consistent resistance predictions. Similar to the analyses for the test database, the codified Q_f function is observed to be more conservative for large absolute values of the n ratio. The Q_f function can be adopted to consider the chord stress effect. It is noted that the numerical database only covers mild steel and θ_1=90°; thus, the corresponding effects of steel material and brace angle for RHS-to-RHS X joints cannot be examined.

It can be concluded that the proposed Lan-Kuhn method gives good correlations with the test data and excellent correlations with the numerical results, and is better than the Kuhn and Lan methods. The proposed modified bearing-buckling method produces nearly equivalent resistance predictions when compared with the proposed Lan-Kuhn method. Thus, it can be adopted as an alternative design method which is in line with the current design rules employing column buckling curves to determine the joint resistance. Although the Yu method is also very accurate, the proposed design methods which give designers more insights into the structural behaviour of RHS joints are easier to use and thus are recommended for RHS-to-RHS X joints. Figs. 5-6 illustrate the comparison of the test and numerical resistances with those predicted by the proposed design methods, both using the C_f factor.

3.5. RHS X joints with only one RHS brace welded to the chord

Table 13 summarises the collated test results totalling 22 RHS X joints with an RHS brace welded to one side of the chord and with the support of a block, a flat plate or a rigid solid base at the opposite side of the chord. It should be noted that although these test specimens have the physical appearance of RHS T joints, the load transfer was comparable to that of an X joint without shear in the chord, and thus these specimens were classified as RHS X joints in line with ISO 14346 [8]. The experimental database consists of test results reported by Barentse [2] for a welded flat plate support, plus Zhao [35], Pandey and Young [36] and Fan [31] for a rigid solid base. The smaller brace width on either chord side was taken as h_1 in Table 13. It is noted that the test results of RHS X joints with an unwelded block support reported by Poloni [37] were not included. This is because the chord cross-sections used had large h_0/t_0 or b_0/t_0 ratios of 57, and hence were potentially sensitive to fabrication tolerances and deviations in the test set-up. The chord wall slenderness is also out of the typical parameter ranges commonly adopted in practice. The RHS X joints with N_{1u}/N_y>1.1 were excluded from the statistical analyses.

For the compiled RHS X joints, Kuhn et al. [21] proposed three conditions of the chord sidewall end-restraint along the chord length direction and corresponding chord sidewall slenderness as follows:

(a) Fixed-fixed: member or plate welded to two opposite chord sides, with a chord sidewall slenderness of $\lambda_{0.5}$.
(b) Fixed-pinned: member or plate welded to one chord side and unwelded to the opposite chord side, with a chord sidewall slenderness of $\lambda_{0.7}=1.4\lambda_{0.5}$.
(c) Pinned-pinned: plates or supports unwelded to two opposite chord sides, with a chord sidewall slenderness of $\lambda_{1.0}=2\lambda_{0.5}$.

According to this classification, the RHS X joints with an RHS brace welded to one chord side and with a plate support welded to the opposite chord side, tested by Barentse [2], can be categorized as class a. Table 14 shows that the mean values of $N_{1u}/N_{P,M}$ and $N_{1u}/N_{P,LK}$ ratios are 1.07 and 1.08, respectively, with corresponding CoVs of 0.054 and 0.059. It is demonstrated that the proposed design methods are applicable for these RHS X joints.

The remaining RHS X joints investigated by Zhao [35], Pandey and Young [36], and Fan [31] using a rigid solid base can be grouped as class b. Thus, a chord sidewall slenderness of $1.4\lambda_{0.5}$ and a buckling curve c were used to derive the buckling reduction factor ($\chi_{P,M1}$) and the joint resistance for the proposed modified bearing-buckling method. For the proposed Lan-Kuhn method, the buckling reduction factor may be obtained from:

$$\chi_{P,LK1} = 1.12\text{-}0.017\frac{h_0}{t_0}\sqrt{\frac{f_{y0}}{355}} \qquad \text{with } h_0/t_0 \le 40(355/f_{y0})^{0.5} \text{ but} \le 40 \qquad (38)$$

It is noted that the buckling reduction factor for RHS X joints in class b decreases non-linearly with increasing h_0/t_0 ratio, for high yield stress and large chord sidewall slenderness. Thus, the validity of the approach of using $1.4\lambda_{0.5}$ and the proposed linearized $\chi_{P,LK1}$ function of Eq. (38) (which can become considerably conservative) has to be limited by $h_0/t_0 \le 40(355/f_{y0})^{0.5}$ but ≤40. The proposed h_0/t_0 limits are 40, 40, 35, 28, 25 and 24 for steel grades of S235, S355, S460, S700, S900 and S960, respectively. Such limits are comparable to the class 3 limit specified in the current EN 1993-1-1 [6], therefore the chord cross-section can be alternatively limited to class 3. This leaves only one RHS X joint for S960, and the results of statistical analyses for the screened test database of class b are shown in Table 15. The mean values of $N_{1u}/N_{P,M}$ and $N_{1u}/N_{P,LK}$ ratios are 1.16 and 1.18, respectively, with corresponding CoVs of 0.130 and 0.141. It is shown that the proposed design methods provide conservative resistance predictions. “RHS X joints” with members unwelded to two opposite chord sides in class c are not examined in this study, but the chord sidewall slenderness of $\lambda_{1.0}$ suggested by Kuhn et al. [21] may be used.

3.6. RHS T and Y joints

Yu [19] conducted numerical simulations on chord sidewall failure in full-width RHS-to-RHS T joints. For the T joints under brace axial compression, the global chord bending at the chord crown was eliminated by applying compensating moments at the chord ends (i.e., Q_f=1.0). The resistance of one full-width RHS-to-RHS T joint with 2γ=24 was 1% higher than that of the comparable x11a specimen (see Table 9), and the same design rules were proposed to be applied to RHS-to-RHS X and T joints. The aforementioned design recommendations developed for RHS X joints are thus suggested for RHS T joints, which is also line with the current design codes and design guides. The approach of only including a term of $(1/\sin\theta_1)^{0.5}$ in the final resistance equation is suggested for RHS Y joints to consider the brace angle effect, which gives unified design rules for RHS X, T and Y joints.

Yu [19] also numerically examined the chord stress effect on RHS-to-RHS X and T joints with varying chord sidewall slenderness and chord stress ratios. It was also shown that the effect of the bending moment could be considered by the Q_f function. The plastic moment resistance ($M_{pl,0,Rd}$) for class 1 or 2 chord cross-sections and the elastic moment resistance ($M_{el,0,Rd}$) for class 3 chord cross-sections could be adopted to calculate the chord stress ratio. Such recommendations will be incorporated in the subsequent proposed design rules in Section 7.

4. Discussion on full-width RHS X and T joints under brace axial tension

Test data of full-width RHS X and T joints subjected to brace axial tension are available for mild steel and high-strength steel in the literature; however, reanalyses of the test results are required. De Koning and Wardenier [38] summarised the up-to-date test results for mild steel up to 1984 and compared the test resistances with those obtained from the resistance equations for chord sidewall failure and brace failure given by Wardenier [29], which are nearly identical to those in the current design codes and design guides. These test results confirm the suitability of the codified design rules for steel grades up to and including S355.

Contradictory research findings have been reported for RHS joints in higher steel grades. For example, for S450 RHS-to-RHS X and T joints, Becque and Wilkinson [39] recommended the use of material factors for RHS joints with non-ductile fracture failure modes. For the full-width X joints, brittle chord corner fracture and brace failure were observed, both with low deformation capacity. In contrast, Björk and Saastamoinen [40] and Tuominen and Björk [41] concluded, based on an assessment of the design equations in EN 1993-1-8 [7], that no material factors are required for RHS-to-RHS X joints using S420 and S460 and the joints could be considered as being ductile. Feldmann et al. [32] suggested material factors of 1.0, 0.90 and 0.80 for steel grades of S500, S700 and S960, respectively. It is noted that the analyses conducted by Feldmann et al. [32] are based on a comparison of the test resistances with the Eurocode design resistances, and no separate statistical analyses per failure mode were conducted. The failure modes observed in tests sometimes deviated from those predicted by EN 1993-1-8 [7], which incorporates different safety factors in the design equations for various failure modes.

It is noted that most of the tests have been carried out for RHS joints with square hollow section (SHS) brace and chord having the same steel grade and wall thickness. Comparison of the resistance equations for the brace effective width failure with those for chord sidewall failure in RHS joints with θ_1=90° shows that the equations then become rather similar. Furthermore, the material softening in the brace and chord resulting from welding could vary and thus may alter the failure location. These factors explain the observed change in failure modes for higher-strength steel joints.

Therefore, more detailed analyses of the aforementioned test results are needed for chord sidewall failure in full-width RHS joints under brace axial tension. The resistance and deformation capacity per failure mode need to be re-evaluated to ascertain whether, for the proposed design methods, lower resistance factors (ϕ) or higher safety factors (γ_M) have to be applied for RHS joints using higher steel grades. Further, it is important that the steel materials used for tests are representative of those in production specifications.

5. Discussion on RHS X and T joints under brace in-plane bending

Table 16 shows the compiled numerical results totalling eight full-width RHS-to-RHS X joints under brace in-plane bending reported by Yu [19]. The numerical resistances ($M_{1u,ip}$) were compared with the yield resistances ($M_{y,ip}$) obtained from:

$$M_{y,ip} = 0.5 f_{y0} t_0 \left(h_1 + 5t_0 \right)^2 Q_f \quad (39)$$

It is shown that all joints, except for the x12ie2 specimen, reach the yield resistance ($M_{y,ip}$), and the resistance ratios ($M_{1u,ip}/M_{y,ip}$) of all joints exceed 1.1 except for the specimens of x11ie2 and x12ie2.

The collated numerical results were adopted to evaluate the six design methods described in Section 3.1. The codified resistance equation (see Eq. (8)) was used. However, the χ_C in Eq. (8) was replaced with $\chi_{0.5}$ for the modified bearing-buckling method ($M_{C,M,ip}$), χ_{Kuhn} (see Eq. (11)) for the Kuhn method ($M_{Kuhn,ip}$), $\chi_{ip,0.5}$ (see Eq. (17)) for the Yu method ($M_{Yu,ip}$) and χ_{Lan} (see Eq. (28)) for the Lan method ($M_{Lan,ip}$). The term of $\chi_C f_{y0}$ in Eq. (8) was replaced with $f_{k,P}$ (see Eq. (33)) for the proposed modified bearing-buckling method ($M_{P,M,ip}$) and the Lan-Kuhn method ($M_{P,LK,ip}$). The Eurocode buckling curve c was conservatively used for all the RHS joints using hot-finished hollow sections.

Table 17 summarises the results of the statistical analyses. It is shown that the Yu method gives lowest CoV of 0.072, and the CoVs of all other design methods are relatively large. However, it would be currently difficult to draw conclusions with respect to the design methods. This is because the $M_{1u,ip}/M_{y,ip}$ ratios of most of the RHS-to-RHS X joints are higher than 1.1. Additionally, for all the design methods, the plastic moment resistance, assuming that the stress within the bearing length of (h_1+5t_0) all reaches the yield stress (f_{y0}), is used and the local buckling effect is considered by the buckling reduction factor. This means that the strain at the outer part of the bearing length would be considerably high, which may result in premature fracture failure for high-strength steel RHS joints. More tests are needed to evaluate the suitability of these design methods for chord sidewall failure in higher-strength steel RHS joints. It has to be examined whether the resistance of high-strength steel joints can be based on a plastic stress distribution.

Yu [19] also reported that the resistances of six full-width RHS-to-RHS T joints under brace in-plane bending were close to those of comparable RHS-to-RHS X joints (i.e., specimens of x10ie05, x10ie, x10ie2, x11ie2, x12i and x12ie2 in Table 16) with a maximum positive deviation of 5%. Thus, it is recommended to adopt the same resistance equations for full-width RHS-to-RHS X and T joints under brace in-plane bending.

Nagui [42] numerically examined the effects of chord sidewall convexity and thickness tolerance on full-width RHS-to-RHS T joints under brace in-plane bending. All the T joints had η*=η=1.0. Table 18 shows a comparison of the numerical resistances ($M_{1u,ip}$) with the predicted resistances ($M_{C,ip}$) obtained from Eq. (8) using χ_C =1.0. The $M_{1u,ip}/M_{C,ip}$ ratio becomes smaller for higher steel grades indicating more significant effects of the fabrication imperfections and more pronounced material effects. This further justifies the use of the material factor (C_f) which could cover these effects for high-strength steel RHS joints.

6. Discussion on RHS X and T joints under brace out-of-plane bending

Table 19 tabulates the collated numerical results totalling eight full-width RHS-to-RHS X joints under brace out-of-plane bending reported by Yu [19]. The numerical resistances ($M_{1u,op}$) were compared with the yield resistances ($M_{y,op}$) derived from:

$$M_{y,op} = f_{y0} t_0 \left(b_0 - t_0\right)\left(h_1 + 5t_0\right) Q_f \tag{40}$$

It is shown that six joints reach the yield resistance ($M_{y,op}$), and the resistance ratios ($M_{1u,op}/M_{y,op}$) of three joints exceed 1.1.

The numerical results were adopted to evaluate the six design methods described in Section 3.1. The codified resistance equation (see Eq. (9)) was used. However, the χ_C in Eq. (9) was replaced with $\chi_{0.5}$ for the modified bearing-buckling method ($M_{C,M,op}$), χ_{Kuhn} (see Eq. (11)) for the Kuhn method ($M_{Kuhn,op}$), $\chi_{0.5}$ for the Yu method ($M_{Yu,op}$) and χ_{Lan} (see Eq. (28)) for the Lan method ($M_{Lan,op}$). The term of $\chi_C f_{y0}$ in Eq. (9) was replaced with $f_{k,P}$ (see Eq. (33)) for the proposed modified bearing-buckling method ($M_{P,M,op}$) and the Lan-Kuhn method ($M_{P,LK,op}$). The Eurocode buckling curve c was conservatively used for all the RHS joints using hot-finished hollow sections. Table 20 shows that the proposed modified bearing-buckling method and the Lan-Kuhn method produce the lowest CoVs of 0.054 and 0.046, respectively. However, similar to the discussion in Section 5, it is currently difficult to draw generalised conclusions with respect to the design methods for the loading case of brace out-of-plane bending. This is because the database is small with three X joints having $M_{1u,op}/M_{y,op}$>1.1, and most of the X joints examined reached the yield resistance. Fracture failure may occur due to the lower material ductility of high-strength steel. More tests, in particular for chord sidewall failure in high-strength steel joints, are thus required.

Yu [19] also numerically studied full-width RHS-to-RHS T joints under brace out-of-plane bending. These joints generally failed by distortion of the chord cross-section, and the corresponding joint resistance and stiffness largely depend on the unstiffened chord length. If chord distortion is prevented, the same resistance equation can be adopted for chord sidewall failure in RHS-to-RHS X and T joints under brace out-of-plane bending.

7. Proposed design rules for RHS joints under brace axial compression

More investigations on chord sidewall failure in high-strength steel RHS joints under brace axial tension, brace in-plane bending and brace out-of-plane bending are needed to assess the design methods comprehensively. Therefore, only design rules for chord sidewall failure in RHS X, T and Y joints under brace axial compression are proposed herein. The numerical study conducted by Yu [19] shows that the resistances of RHS-to-RHS T joints with n=0 are slightly higher than those of comparable RHS-to-RHS X joints. The approach of only including a term of $(1/\sin\theta_1)^{0.5}$ in the final resistance equation is suggested for RHS X, T and Y joints in this study because of the similar structural behaviour of these joints. Thus, the results of statistical analyses for X joints can be considered to be also representative for T and Y joints. The proposed design methods using the recommended C_f factor can provide conservative resistance predictions for full-width RHS X joints with only one RHS brace welded to one chord side. For such RHS joints, the $\chi_{P,M}$ or $\chi_{P,LK}$ are appropriate for a welded plate (or similar) on the other chord side (class a joints), and the proposed $\chi_{P,M1}$ or $\chi_{P,LK1}$ are suitable for an unwelded support on the other chord side (class b joints). Hence, only the results of statistical analyses for RHS-to-RHS X joints under brace axial compression were adopted to evaluate the mean resistance to the design resistance for the proposed design methods.

AISC 360-16 [43] stipulates a reliability index of 3.0 for ductile welded hollow section joints and often adopts the simplified Eq. (41) from Ravindra and Galambos [44] to derive the resistance factor (ϕ). The beneficial overall effects of variations of geometric parameters and material properties are neglected in the calibration.

$$\phi = (\text{Mean})e^{(-0.55)(3.0)(\text{CoV})} \tag{41}$$

Table 8 shows that the mean values of the $N_{1u}/N_{P,M}$ and $N_{1u}/N_{P,LK}$ ratios are 1.17 and 1.17, respectively, with corresponding CoVs of 0.091 and 0.095 for the evaluation against the test database. The corresponding obtained ϕ factors are 1.01 and 1.00. For the assessment against the numerical database (see Table 12), the mean values of the $N_{1u}/N_{P,M}$ and $N_{1u}/N_{P,LK}$ ratios are 1.23 and 1.24, respectively, with corresponding CoVs of 0.065 and 0.064. The corresponding derived ϕ factors are 1.10 and 1.12. Thus, the smaller ϕ factors obtained from the evaluation against the test results are governing and a rounded-off ϕ factor of 1.0 can be adopted for the two proposed design methods. This indicates that the proposed modified bearing-buckling method and the Lan-Kuhn method produce equivalent nominal and design resistances.

Both the proposed modified bearing-buckling method and the Lan-Kuhn method adopt chord sidewall slenderness according to the conditions of chord sidewall end-resistant, an angle function of $(1/\sin\theta_1)^{0.5}$ in the final resistance equation, an $(\eta^*)^{-0.15}$ correction in the f_k function and a buckling curve c or equivalent. Tables 21-22 summarise the design rules using the two proposed design methods. It should be noted that for plate-to-RHS X joints and RHS-to-RHS X joints with $h_1/h_0 \leq 0.25$, $f_k=f_{y0}$ is suggested in line with Kuhn et al. [21]; however, the nominal f_{y0} values should not exceed 460 MPa due to the lack of test data for high-strength steel RHS joints.

8. Conclusions

This study deals with the design of chord sidewall failure in rectangular hollow section (RHS) X, T and Y joints.

Test and numerical results reported in the literature for chord sidewall failure in RHS joints were collated. A wide range of geometric parameters, steel grades up to S960 and loading cases of brace axial loading, brace in-plane bending and brace out-of-plane bending were investigated. The effects of brace-to-chord height ratio (η*), brace angle (θ_1), chord stress ratio (n) and steel grade were evaluated. The representative existing design approaches and two proposed design methods were evaluated against the compiled test and numerical results. Further required research on, in particular, high-strength steel RHS joints under brace axial tension, brace in-plane bending and brace out-of-plane bending, was discussed. The conclusions for the loading case of brace axial compression are summarised as follows:

(1) The effect of the η* ratio on the joint resistance is pronounced and incorporating a correction term of $(\eta^*)^{-0.15}$ in the buckling stress function (f_k) significantly reduces the scatter of resistance predictions.

(2) The approach of only including a term of $(1/\sin\theta_1)^{0.5}$ in the final resistance equation can more accurately quantify the effect of brace angles and is recommended.

(3) The current codified chord stress function (Q_f) becomes more conservative for large absolute values of the n ratio and can be used to provide lower bound predictions for the chord stress effect.

(4) An equation for the material factor (C_f) is suggested to consider the material effect; the rounded-off C_f values are 1.0, 0.95, 0.90, 0.85 and 0.80 for steel grades of S355, S460, S700, S900 and S960, respectively.

(5) The proposed modified bearing-buckling method and the simpler Lan-Kuhn method provide more consistent resistance predictions when compared with the existing design methods.

(6) Tables 21-22, which are based on the two proposed alternative design methods, summarise the proposed design rules for chord sidewall failure, which consider varying conditions of the chord sidewall end-restraint, with a resulting resistance factor (ϕ) of 1.0.

Acknowledgements

The authors are grateful to Mr. J. Kuhn at Schlaich Bergermann Partner for making his data files available and to Dr. Fleischer at KoRoH GmbH-CCTH for being so kind as to perform, in an initial phase, reliability analyses of the data using the Eurocode procedure. Appreciation is also extended to Dr. Y. Yu at Allseas for her detailed and critical review.

References

[1] Czechowski J., Brodka J., Etude de la resistance statique des assemblages soudes en croix de profils creux rectangulaires. Constr. Metallique 3 (1977) 17-25.

[2] Barentse J., Investigation into the static strength of welded T-joints made of rectangular hollow sections. Stevin Reports 6-76-23 and 6-77-7, Delft University of Technology, The Netherlands, 1977.

[3] Brodka J., Szlendak J., Strength of cross joints in rectangular hollow sections. XXVI scientific conference of the civil and hydraulic engineering section of the Polish academy of science and of the science division of PZITB, 1980.

[4] Kato B., Nishiyama I., The static strength of RR-joints with large b/B ratio. IIW Doc. XV-459-80, 1980.

[5] Wardenier J., Davies G., The strength of predominantly statically loaded joints with a square or rectangular hollow section chord. IIW Doc. XV-462-81, 1981.

[6] Eurocode 3 (EC3), Design of steel structures-Part 1-1: General rules and rules for buildings, EN 1993-1-1. European Committee for Standardization, CEN, Brussels, Belgium, 2005.

[7] Eurocode 3 (EC3), Design of steel structures-Part 1-8: Design of joints, EN 1993-1-8. European Committee for Standardization, CEN, Brussels, Belgium, 2005.

[8] Static design procedure for welded hollow-section joints-Recommendations, ISO/FDIS 14346. International Standardization Organization, ISO, Geneva, Switzerland, 2013.

[9] Packer J.A., Wardenier J., Kurobane Y., Dutta D., Yeomans N., Design guide for rectangular hollow section (RHS) joints under predominantly static loading, 1st Ed., CIDECT, Verlag TUV Rheinland, Cologne, Germany, 1992.

[10] Packer J.A., Wardenier J., Zhao X.L., van der Vegte G.J., Kurobane Y., Design guide for rectangular hollow section (RHS) joints under predominantly static loading, 2nd Ed., CIDECT, Geneva, Switzerland, 2009.

[11] Design recommendations for hollow section joints-Predominantly statically loaded, 1st Ed., International Institute of Welding (IIW), Subcommission XV-E, Rev. IIW Doc. XV-491-81, 1981.

[12] Design recommendations for hollow section joints-Predominantly statically loaded, 2nd Ed., International Institute of Welding (IIW), Subcommission XV-E, IIW Doc. XV-701-89, 1989.

[13] Static design procedure for welded hollow section joints-Recommendations, 3rd Ed., International Institute of Welding (IIW), Subcommission XV-E, IIW Doc. XV-1402-12, 2012.

[14] Davies G., Packer J.A., Coutie M.G., The behavior of full width RHS cross joints. Proceedings of IIW international conference on welding of tubular structures, Boston, U.S.A, 1984.

[15] Packer J.A., Web crippling of rectangular hollow sections. J. Struct. Eng. 110 (10) (1984) 2357-2373.

[16] Giddings T.W., Wardenier J., The strength and behaviour of statically loaded welded connections in structural hollow sections, CIDECT Monograph 6, 1986.

[17] Davies G., Roodbaraky K., The effect of angle on the strength of RHS joints. Proceedings of the international meeting on safety criteria in design of tubular structures, Tokyo, Japan, 1987.

[18] Platt J.C., Sidewall behaviour in full-width rectangular hollow section joints. PhD thesis, University of Nottingham, Nottingham, U.K, 1984.

[19] Yu Y., The static strength of uniplanar and multiplanar connections in rectangular hollow sections. PhD thesis,

Delft University of Technology, Delft, The Netherlands, 1997.

[20] Becque J., Cheng S., Sidewall buckling of equal-width RHS truss X-joints. J. Struct. Eng. 143(2) (2016) 04016179.

[21] Kuhn J., Packer J.A., Fan Y.J., RHS webs under transverse compression. Can. J. Civ. Eng. 46 (2019) 810-827.

[22] Wardenier J., Minutes of IIW Subcommission XV-E meeting, Singapore, IIW Doc. XV-E 482c-19, 2019.

[23] Lan X.Y., Chan T.M., Young B., Structural behaviour and design of high strength steel RHS X-joints. Eng. Struct. 200 (2019) 109494.

[24] Lan X.Y., Chan T.M., Young B., Testing, finite element analysis and design of high strength steel RHS T-joints. Eng. Struct. 227 (2020) 111184.

[25] Eurocode 3 (EC3), Design of steel structures-Part 1-8: Design of joints, prEN 1993-1-8. European Committee for Standardization, CEN, Brussels, Belgium, 2019.

[26] Wardenier J., Vegte G.J. van der, Liu, D.K., Chord stress function for rectangular hollow section X and T joints. Proceedings 17th International Offshore and Polar Engineering Conference, Lisbon, Portugal, 2007.

[27] Lan X.Y., Chan T.M., Young B., Structural behaviour and design of chord plastification in high strength steel CHS X-joints. Constr. Build. Mater. 191 (2018) 1252-1267.

[28] Lan X.Y., Chan T.M., Young B., Structural behaviour and design of high strength steel CHS T-joints. Thin Wall. Struct. https://doi.org/10.1016/j.tws.2020.107215.

[29] Wardenier J., Hollow Section Joints. Delft University Press, The Netherlands, 1982.

[30] Wardenier J., Lan X.Y., Packer J.A., Evaluation of design methods for chord sidewall failure in RHS joints using steel grades up to S960-state of the art. IIW Doc. XV-E-489-20, 2020.

[31] Fan Y., RHS-to-RHS axially loaded X-connections offset towards an open chord end. Master thesis, University of Toronto, Toronto, Canada, 2017.

[32] Feldmann M., Schillo N., Schaffrath S., Virdi K., Björk T., Tuominen N., Veljkovic M., Pavlovic M., Manoleas P., Heinisuo M., Mela K., Ongelin P., Valkonen I., Minkkinen J., Erkkilä J., Pétursson E., Clarin M., Seyr A., Horváth L., Kövesdi B., Turán P., Somodi B., Rules on high strength steel, Luxembourg, Publications Office of the European Union, 2016.

[33] Pandey M., Young B., Structural performance of cold-formed high strength steel tubular X-joints under brace axial compression. Eng. Struct. 208 (2020) 109768.

[34] Kim S.H, Lee C.H., Shin D.J., Chord stress effect in high-strength steel tubular X-joints. Proceedings 17th International Symposium on Tubular Structures, Singapore, 2019.

[35] Zhao X.L., Deformation limit and ultimate strength of welded T-joints in cold-formed RHS sections. J. Constr. Steel Res. 53 (2000) 149-165.

[36] Pandey M., Young B., Compression capacities of cold-formed high strength steel tubular T-joints. J. Constr. Steel Res. 162 (2019) 105650.

[37] Poloni T., The effect of bearing length on transversely compressed RHS. Bachelor thesis, University of Toronto, Toronto, Canada, 1985.

[38] De Koning C.H.M., Wardenier J., The static strength of welded joints between structural hollow sections or between structural hollow sections and H-sections, Part 2 - Joints between rectangular hollow sections. Delft University of Technology, Stevin report 6-84-19, Delft, The Netherlands, 1985.

[39] Becque J., Wilkinson T., The capacity of grade C450 cold-formed rectangular hollow section T and X connections: an experimental investigation. J. Constr. Steel Res. 133 (2017) 345-359.

[40] Björk T., Saastamoinen H., Capacity of CFRHS X joints made of double grade S420 steel. Proceedings 14th International Symposium on Tubular Structures, London, U.K, 2012.

[41] Tuominen N., Björk T., Capacity of RHS-joints made of high strength steels. CIDECT Report 5BZ, Lappeenranta University of Technology, Finland, 2016.

[42] Nagui A., A comparative analysis of the resistance of tubular joints. Master thesis, University of Bologna, Italy, 2016.

[43] Specification for structural steel buildings. American Institute of Steel Construction (AISC), ANSI/AISC 360-16, Chicago, U.S.A, 2016.

[44] Ravindra M.K., Galambos T.V., Load and resistance factor design for steel. J. Struct. Div. 104 (ST9) (1978) 1337-1353.

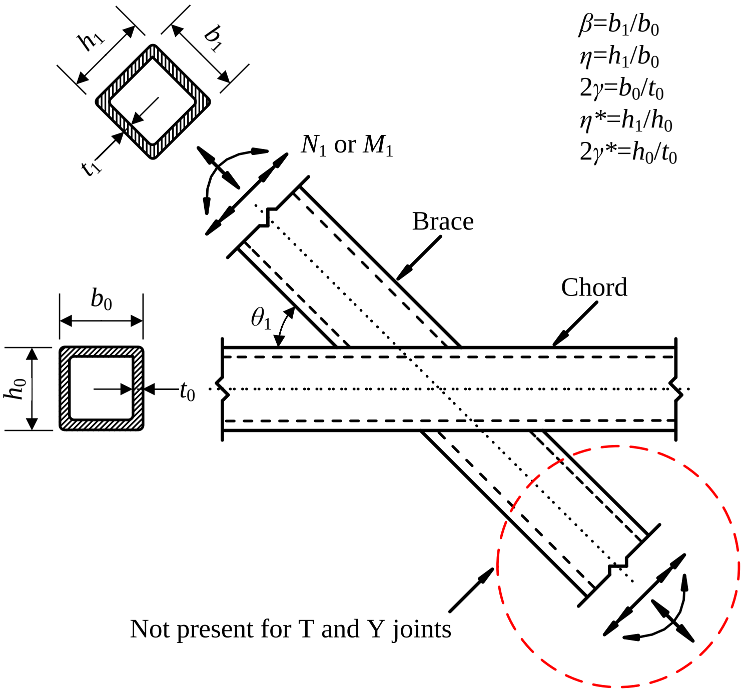

Fig. 1. Configurations and notations of RHS-to-RHS X, T and Y joints.

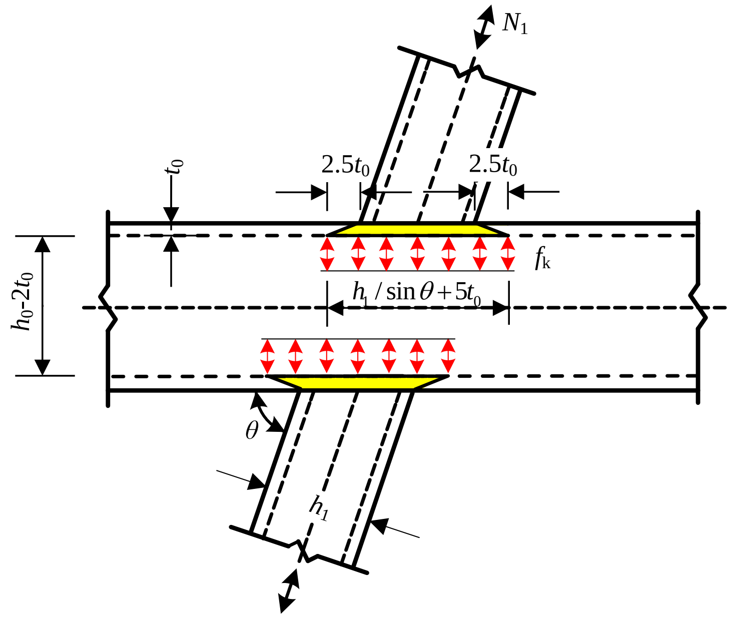

Fig. 2. Codified bearing-buckling model for chord side wall failure.

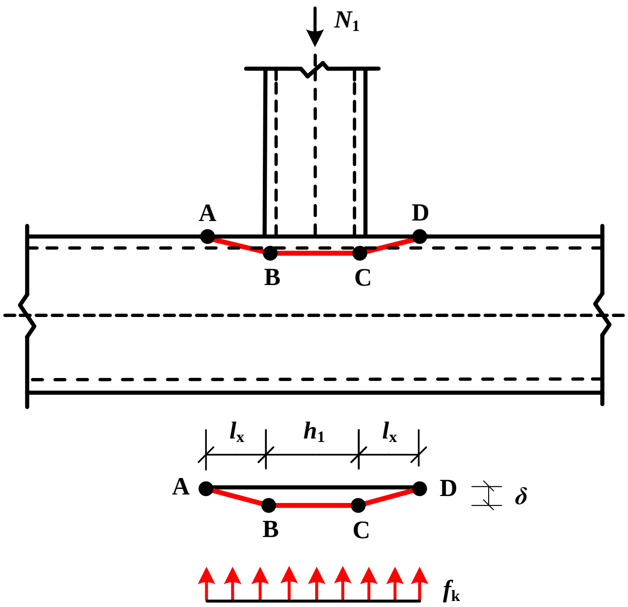

Fig. 3. Four-hinge yield line model proposed by Yu [19].

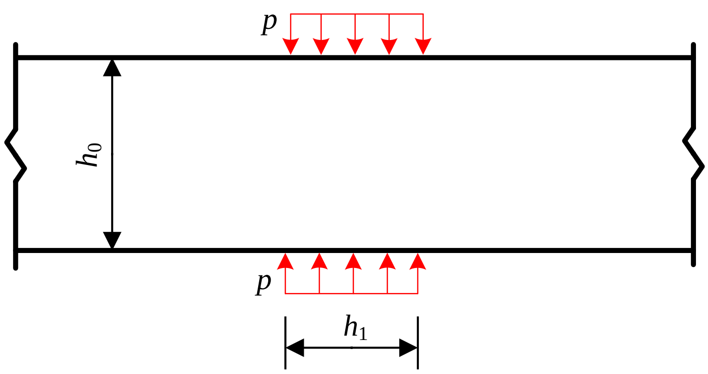

Fig. 4. Plate buckling model proposed by Lan et al. [23-24].

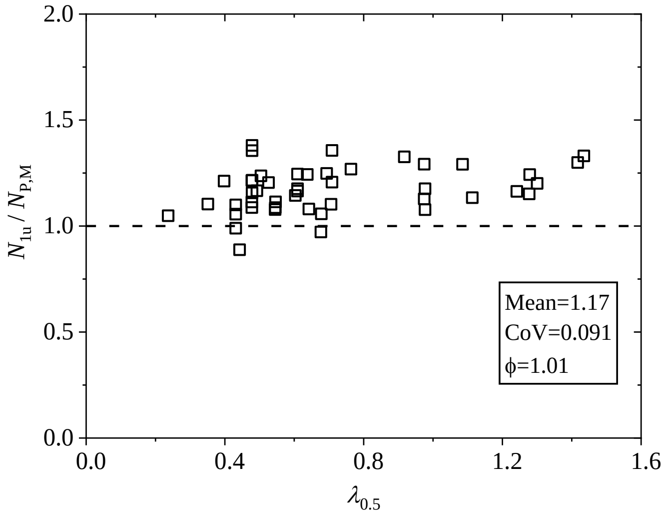

(a) Modified bearing-buckling method

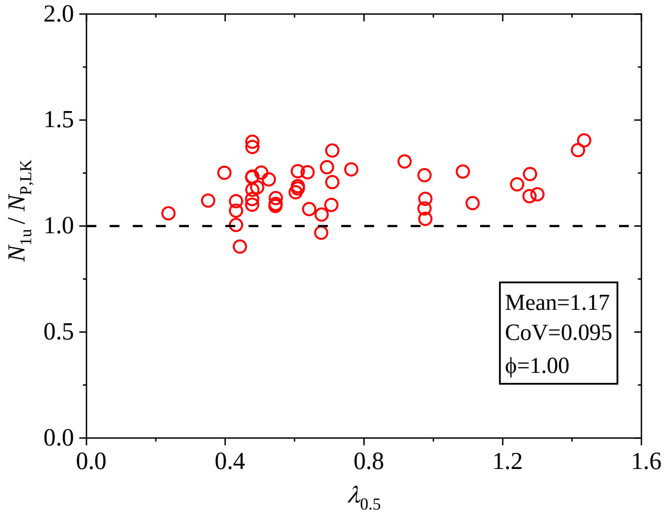

(b) Lan-Kuhn method

Fig. 5. Comparison of test resistances of 46 RHS-to-RHS joints under brace axial compression with those predicted by the proposed design methods, using the C_f factor.

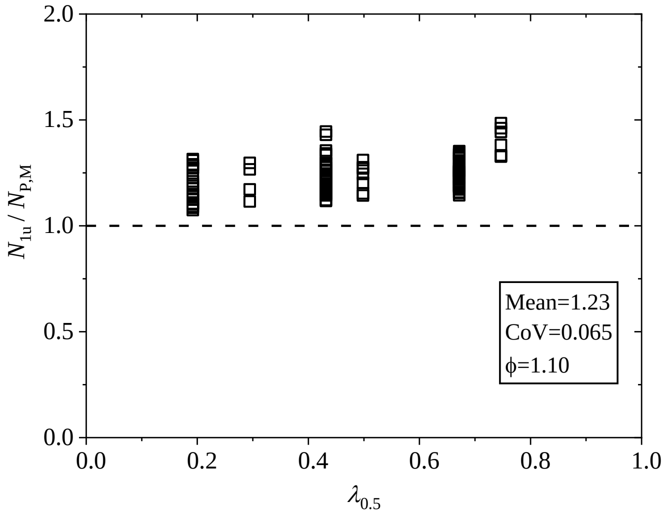

(a) Modified bearing-buckling method

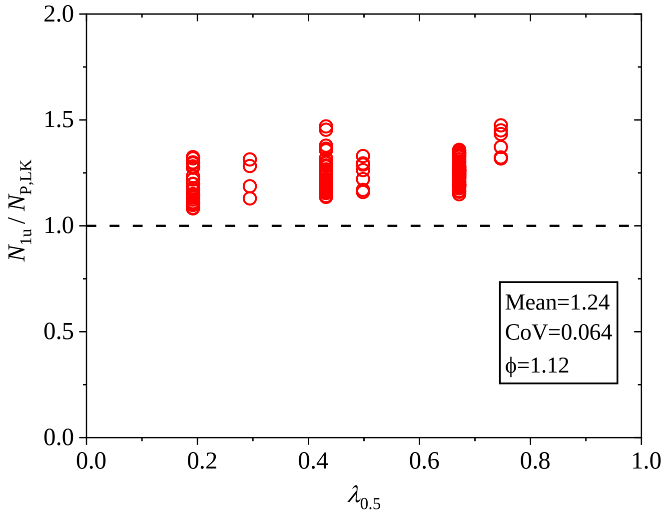

(b) Lan-Kuhn method

Fig. 6. Comparison of numerical resistances of 131 RHS-to-RHS joints under brace axial compression with those predicted by the proposed design methods, using the C_f factor.

Table 1

Codified design resistance for chord side wall failure in mild steel RHS joints with β=1.0 [8, 10, 13].

<table>
<tr><th>T, Y and X joints</th><th colspan="2">Brace axial loading</th></tr>
<tr><td rowspan="11">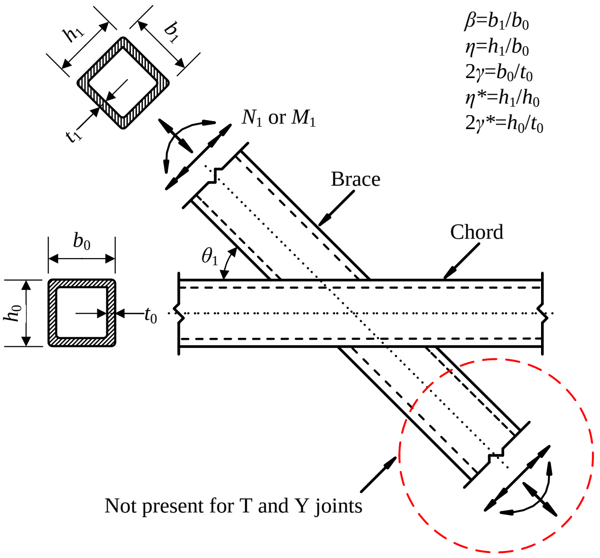
</td>
<td rowspan="2">$N_{1,\mathrm{Rd}} = \frac{f_k t_0}{\sin\theta_1}\left(\frac{2h_1}{\sin\theta_1} + 10t_0\right)Q_f$</td><td>Tension: $f_k = f_{y0}$</td></tr>
<tr><td>Compression:
$f_k = \chi_C f_{y0}$ for T and Y joints
$f_k = 0.8\chi_C f_{y0}\sin\theta_1$ for X joints</td></tr>
<tr><td colspan="2">Brace in-plane bending</td></tr>
<tr><td>$M_{ip,1,\mathrm{Rd}} = 0.5 f_k t_0 \left(h_1 + 5t_0\right)^2 Q_f$</td><td>$f_k = f_{y0}$ for T and Y joints
$f_k = 0.8\chi_C f_{y0}$ for X joints</td></tr>
<tr><td colspan="2">Brace out-of-plane bending</td></tr>
<tr><td>$M_{op,1,\mathrm{Rd}} = f_k t_0 (b_0 - t_0)(h_1 + 5t_0) Q_f$</td><td>$f_k = \chi_C f_{y0}$ for T and Y joints
$f_k = 0.8\chi_C f_{y0}$ for X joints</td></tr>
<tr><td colspan="2">Parameters</td></tr>
<tr><td colspan="2">where χ_C is the reduction factor for column buckling according to e.g., EN 1993-1-1 [6] using the relevant buckling curves and a normalised slenderness defined by:
$$\lambda_C = \frac{3.46\left(\frac{h_0}{t_0} - 2\right)\sqrt{\frac{1}{\sin\theta_1}}}{\pi\sqrt{\frac{E}{f_{y0}}}}$$</td></tr>
<tr><td colspan="2">$Q_f = (1 - |n|)^{0.1}$ with n in connecting chord face
$n = \frac{N_{0,\mathrm{Ed}}}{N_{pl,0,\mathrm{Rd}}} + \frac{M_{0,\mathrm{Ed}}}{M_{pl,0,\mathrm{Rd}}}$ for class 1 or 2 chord cross-sections under chord compression stress and for chord cross-sections under chord tension stress</td></tr>
<tr><td colspan="2">Validity ranges</td></tr>
<tr><td colspan="2">steel grades up to S355; $b_0/t_0 \leq 40$, $h_0/t_0 \leq 40$, the chord cross-section shall be class 1 or 2 for the chord under compression stress; $0.5 \leq h_0/b_0 \leq 2.0$; $\theta_1 \geq 30°$.</td></tr>
</table>

Table 2

Comparison of buckling reduction factors for RHS joints with h_1/h_0=1.0 and θ_1=90°.

f_{y0} (MPa)	h_0/t_0	$\chi_{P,M}$	$\chi_{P,LK}$	χ_{Kuhn}	χ_{Lan}	$\chi_{P,LK}/\chi_{P,M}$	$\chi_{Kuhn}/\chi_{P,M}$	$\chi_{Lan}/\chi_{P,M}$
960	10	0.95	0.92	0.93	1.00	0.97	0.98	1.05
	20	0.74	0.73	0.72	0.86	0.98	0.97	1.16
	30	0.52	0.53	0.50	0.60	1.02	0.98	1.16
	35	0.42	0.43	0.40	0.47	1.02	0.94	1.12
	40	0.34	0.33	0.29	0.34	0.96	0.84	0.98
700	10	0.97	0.95	0.97	1.00	0.98	0.99	1.03
	20	0.80	0.78	0.78	0.94	0.98	0.98	1.17
	30	0.61	0.61	0.60	0.72	1.01	0.99	1.18
	40	0.43	0.45	0.41	0.49	1.04	0.96	1.14
460	10	1.00	0.98	1.00	1.00	0.99	1.00	1.00
	20	0.86	0.85	0.85	1.00	0.98	0.99	1.16
	30	0.71	0.71	0.70	0.84	1.00	0.99	1.19
	40	0.55	0.57	0.55	0.66	1.04	1.00	1.20
355	10	1.00	1.00	1.00	1.00	1.00	1.00	1.00
	20	0.89	0.88	0.89	1.00	0.99	0.99	1.12
	30	0.77	0.76	0.76	0.91	0.99	0.99	1.19
	40	0.62	0.64	0.63	0.75	1.03	1.00	1.20
235	10	1.00	1.02	1.00	1.00	1.02	1.00	1.00
	20	0.93	0.92	0.94	1.00	0.99	1.00	1.07
	30	0.83	0.83	0.83	1.00	0.99	1.00	1.20
	40	0.72	0.73	0.72	0.87	1.01	1.00	1.20
Max						1.04	1.00	1.20
Min						0.96	0.84	0.98
Mean						1.00	0.98	1.12
CoV						0.023	0.036	0.070

Table 3
Collated test results totalling 51 RHS-to-RHS X joints under brace axial compression.

Researcher/year	Specimen	b_0 (mm)	h_0 (mm)	t_0 (mm)	b_1 (mm)	h_1 (mm)	t_1 (mm)	f_{y0} (MPa)	θ_1 (°)	n	η*	2γ*	N_{1u} (kN)	N_{1u}/N_y
Davies/1982	X(3)RR90	100.0	100.0	3.97	100.0	100.0	4.00	320	90	0	1.00	25.2	353	1.16
	X(4)RR45	100.0	100.0	3.93	100.0	100.0	4.00	320	45	0	1.00	25.4	372	1.04
Platt/1982	X-RR-90-A	100.0	100.2	4.20	100.0	100.0	4.00	432	90	0	1.00	23.9	391	0.89
	X-RR-60-A	99.8	100.1	4.20	100.0	100.0	4.00	432	60	0	1.00	23.8	410	0.87
	X-RR-45-A	100.1	100.0	4.20	100.0	100.0	4.00	432	45	0	1.00	23.8	450	0.86
	X-RR-90-B	98.7	100.0	4.00	100.0	50.0	5.00	311	90	0	0.50	25.0	209	1.20
	X-RR-60-B	98.9	100.0	4.10	100.0	50.0	5.00	311	60	0	0.50	24.4	218	1.13
	X-RR-45-B	99.2	100.0	4.00	100.0	50.0	5.00	311	45	0	0.50	25.0	244	1.18
	X-RR-90-C	250.0	251.1	6.50	250.0	250.0	6.30	237	90	0	1.00	38.6	680	0.78
	X-RR-60-C	250.4	250.7	6.50	250.0	250.0	6.30	237	60	0	1.00	38.6	672	0.72
	X-RR-45-C	251.2	250.4	6.70	250.0	250.0	6.30	228	45	0	1.00	37.4	846	0.82
Peksa/1982	10P	99.2	99.2	4.00	99.2	99.2	4.00	304	90	0	1.00	24.8	276	0.95
	11P	99.3	99.3	4.00	99.3	99.3	4.00	304	90	-0.43	1.00	24.8	271	0.93
	12P	99.3	99.3	4.00	99.3	99.3	4.00	304	90	-0.87	1.00	24.8	275	0.95
	13P	99.3	99.3	4.00	99.3	99.3	4.00	304	90	-0.87	1.00	24.8	280	0.97
	14P	99.2	99.2	4.00	99.2	99.2	4.00	304	90	-0.65	1.00	24.8	271	0.93
	15P	99.2	99.2	4.00	99.2	99.2	4.00	304	90	-0.22	1.00	24.8	263	0.91
Bettison/1982	5B	99.6	99.6	4.20	99.6	99.6	4.20	336	90	-0.71	1.00	23.7	313	0.92
	6B	99.8	99.8	4.10	99.8	99.8	4.10	336	90	-0.76	1.00	24.3	284	0.86
Poloni/1985	PWLR	102.4	252.7	4.44	102.4	252.7	4.44	388	90	0	1.00	56.9	438	0.46
Dixon/1983	DD1121	101.7	77.6	5.08	101.7	77.6	5.08	301	90	0	1.00	15.3	403	1.28
	DD1122	77.8	101.8	4.93	77.8	101.8	4.93	370	90	0	1.00	20.6	445	0.96
	DD1222	77.8	101.8	4.93	77.8	101.8	4.93	370	45	0	1.00	20.6	476	0.87
	DD1322	77.8	101.8	4.93	77.8	101.8	4.93	370	60	0	1.00	20.6	459	0.93
	DD2121	304.4	204.1	7.21	304.4	204.1	7.21	406	90	0	1.00	28.3	1315	0.93
	DD2122	204.1	304.4	7.21	204.1	304.4	7.21	406	90	0	1.00	42.2	1230	0.62
	DD2222	204.1	304.4	7.21	204.1	304.4	7.21	406	45	0	1.00	42.2	1675	0.71
	DD3121	203.2	153.6	4.83	203.2	153.6	4.83	392	90	0	1.00	31.8	649	0.97
	DD3122	153.6	203.2	4.83	153.6	203.2	4.83	412	90	0	1.00	42.1	530	0.59
	DD3221	203.2	153.6	4.83	203.2	153.6	4.83	392	44	0	1.00	31.8	693	0.86
	DD3222	153.6	203.2	4.83	153.6	203.2	4.83	412	44	0	1.00	42.1	694	0.64
	DD4123	254.1	254.1	9.35	254.1	254.1	9.35	406	90	0	1.00	27.2	2183	0.96
	DD4223	254.1	254.1	9.35	254.1	254.1	9.35	406	45	0	1.00	27.2	2429	0.90
	DD4323	254.1	254.1	9.35	254.1	254.1	9.35	406	60	0	1.00	27.2	2215	0.90
Cheng/2016	X1	100.5	100.3	2.92	100.2	100.3	2.73	330	90	0	1.00	34.3	176	0.79
	X2	100.4	100.1	3.84	100.4	100.2	3.69	330	90	0	1.00	26.1	302	1.00
	X3	100.3	99.8	4.89	100.1	99.9	4.70	400	90	0	1.00	20.4	373	0.77
	X4	99.6	99.6	5.80	99.8	99.7	5.46	370	90	0	1.00	17.2	560	1.01
	X5	99.9	99.7	7.92	100.1	99.6	7.68	345	90	0	1.00	12.6	783	1.03
	X6	149.8	250.0	5.00	150.1	150.1	4.76	463	90	0	0.60	50.0	409	0.50
	X7	150.2	150.2	5.86	150.5	150.4	5.86	451	90	0	1.00	25.6	828	0.87
	X9	300.0	400.0	7.92	300.3	300.3	7.97	481	90	0	0.75	50.5	1289	0.50
Pandey/2020	X-100×50×4-100×50×4	100.6	50.5	3.97	100.6	50.6	3.97	952	90	0	1.00	12.7	482	0.91
	X-120×120×4-120×120×4	121.6	121.7	3.93	121.4	121.8	3.92	971	90	0	1.00	31.0	567	0.53
	X-140×140×4-140×140×4	140.4	141.5	3.99	141.6	140.4	4.00	1008	90	0	0.99	35.5	484	0.37
	X-120×120×3-120×120×3	120.8	120.4	3.12	120.7	120.3	3.11	1038	90	0	1.00	38.6	317	0.36
	X-80×80×4-80×80×4	80.2	80.4	3.98	80.4	80.2	3.97	1004	90	0	1.00	20.2	595	0.74
	X-120×120×4-120×120×3	120.4	120.8	3.09	121.1	121.4	3.95	1038	90	0	1.00	39.1	318	0.36
Björk/2015	X5-S500	150.0	150.0	5.15	150.0	150.0	5.15	548	90	0	1.00	29.1	815	0.82
	X5-S700	150.0	150.0	5.06	150.0	150.0	5.06	762	90	0	1.00	29.6	935	0.69
	X5-S960	150.0	150.0	4.97	150.0	150.0	4.97	1080	90	0	1.00	30.2	808	0.43

Table 4

Evaluation of design methods with the angle functions in $\lambda_{0.5}$, f_k and the final resistance equations.

Specimen	f_{y0} (MPa)	θ_1 (°)	η*	2γ*	N_{1u} (kN)	$N_{1u}/N_{C,M}$	N_{1u}/N_{Yu}	N_{1u}/N_{Kuhn}	N_{1u}/N_{Lan}	$N_{1u}/N_{P,M}$	$N_{1u}/N_{P,LK}$
X(4)RR45	320	45	1.00	25.4	372	1.17	1.04	1.19	0.92	1.17	1.11
X-RR-90-A	432	90	1.00	23.9	391	1.09	1.02	1.11	0.92	1.09	1.11
X-RR-60-A	432	60	1.00	23.8	410	1.04	0.96	1.06	0.85	1.04	1.03
X-RR-45-A	432	45	1.00	23.8	450	1.01	0.90	1.03	0.79	1.01	0.95
X-RR-90-C	237	90	1.00	38.6	680	1.06	0.97	1.06	0.88	1.06	1.05
X-RR-60-C	237	60	1.00	38.6	672	0.96	0.87	0.96	0.77	0.96	0.92
X-RR-45-C	228	45	1.00	37.4	846	1.04	0.93	1.05	0.79	1.04	0.94
DD1122	370	90	1.00	20.6	445	1.10	1.07	1.10	0.96	1.10	1.11
DD1322	370	60	1.00	20.6	459	1.02	0.97	1.04	0.88	1.02	1.02
DD1222	370	45	1.00	20.6	476	0.93	0.85	0.94	0.77	0.93	0.89
DD4123	406	90	1.00	27.2	2183	1.23	1.14	1.24	1.03	1.23	1.24
DD4323	406	60	1.00	27.2	2215	1.14	1.04	1.16	0.93	1.14	1.11
DD4223	406	45	1.00	27.2	2429	1.11	0.99	1.13	0.85	1.11	1.02
DD3121	392	90	1.00	31.8	649	1.34	1.21	1.35	1.13	1.34	1.34
DD3221	392	44	1.00	31.8	693	1.18	1.02	1.19	0.87	1.18	1.04
DD2122	406	90	1.00	42.2	1230	1.11	1.06	1.10	0.92	1.11	1.07
DD2222	406	45	1.00	42.2	1675	1.35	1.24	1.37	0.92	1.35	1.06
DD3122	412	90	1.00	42.1	530	1.06	1.00	1.05	0.88	1.06	1.02
DD3222	412	44	1.00	42.1	694	1.23	1.12	1.26	0.83	1.23	0.96
Mean						1.11	1.02	1.13	0.89	1.11	1.05
CoV						0.103	0.103	0.105	0.101	0.103	0.104

Note: The material factor (C_f) was not used for all design methods.

Table 5

Evaluation of design methods only including a function of $(1/\sin\theta_1)^{0.5}$ in the final resistance equation.

Specimen	f_{y0} (MPa)	θ_1 (°)	η^*	$2\gamma^*$	N_{1u} (kN)	$N_{1u}/N_{C,M}$	N_{1u}/N_{Yu}	N_{1u}/N_{Kuhn}	N_{1u}/N_{Lan}	$N_{1u}/N_{P,M}$	$N_{1u}/N_{P,LK}$
X(4)RR45	320	45	1.00	25.4	372	1.24	1.16	1.25	1.04	1.24	1.25
X-RR-90-A	432	90	1.00	23.9	391	1.09	1.02	1.11	0.92	1.09	1.11
X-RR-60-A	432	60	1.00	23.8	410	1.06	1.00	1.08	0.90	1.06	1.08
X-RR-45-A	432	45	1.00	23.8	450	1.05	0.99	1.07	0.89	1.05	1.07
X-RR-90-C	237	90	1.00	38.6	680	1.06	0.97	1.06	0.88	1.06	1.05
X-RR-60-C	237	60	1.00	38.6	672	0.97	0.89	0.97	0.81	0.97	0.97
X-RR-45-C	228	45	1.00	37.4	846	1.08	0.99	1.08	0.90	1.08	1.08
DD1122	370	90	1.00	20.6	445	1.10	1.07	1.10	0.96	1.10	1.11
DD1322	370	60	1.00	20.6	459	1.05	1.03	1.06	0.93	1.05	1.07
DD1222	370	45	1.00	20.6	476	0.99	0.96	0.99	0.87	0.99	1.00
DD4123	406	90	1.00	27.2	2183	1.23	1.14	1.24	1.03	1.23	1.24
DD4323	406	60	1.00	27.2	2215	1.16	1.08	1.17	0.98	1.16	1.17
DD4223	406	45	1.00	27.2	2429	1.15	1.07	1.16	0.97	1.15	1.16
DD3121	392	90	1.00	31.8	649	1.34	1.21	1.35	1.13	1.34	1.34
DD3221	392	44	1.00	31.8	693	1.19	1.07	1.21	1.00	1.19	1.19
DD2122	406	90	1.00	42.2	1230	1.11	1.06	1.10	0.92	1.11	1.07
DD2222	406	45	1.00	42.2	1675	1.27	1.21	1.26	1.06	1.27	1.22
DD3122	412	90	1.00	42.1	530	1.06	1.00	1.05	0.88	1.06	1.02
DD3222	412	44	1.00	42.1	694	1.16	1.09	1.15	0.96	1.16	1.11
Mean						1.12	1.05	1.13	0.95	1.12	1.12
CoV						0.086	0.079	0.087	0.082	0.086	0.085

Note: The material factor (C_f) was not used for all design methods.

Table 6
Evaluation of the chord stress effect against test results of eight RHS-to-RHS X joints.

Specimen	f_{y0} (MPa)	θ_1 (°)	n	η*	N_{1u} (kN)	$N_{1u}/N_{C,M}$	N_{1u}/N_{Yu}	N_{1u}/N_{Kuhn}	N_{1u}/N_{Lan}	$N_{1u}/N_{P,M}$	$N_{1u}/N_{P,LK}$
10P	304	90	0	1.00	276	1.11	1.04	1.12	0.95	1.11	1.13
11P	304	90	-0.43	1.00	271	1.16	1.08	1.16	0.99	1.16	1.17
12P	304	90	-0.87	1.00	275	1.36	1.27	1.36	1.16	1.36	1.37
13P	304	90	-0.87	1.00	280	1.38	1.29	1.39	1.18	1.38	1.40
14P	304	90	-0.65	1.00	271	1.21	1.14	1.22	1.04	1.21	1.23
15P	304	90	-0.22	1.00	263	1.09	1.02	1.09	0.93	1.09	1.10
5B	336	90	-0.71	1.00	313	1.22	1.14	1.23	1.04	1.22	1.23
6B	336	90	-0.76	1.00	284	1.17	1.09	1.18	0.99	1.17	1.18
Mean						1.21	1.13	1.22	1.03	1.21	1.23
CoV						0.088	0.088	0.088	0.089	0.088	0.088

Note: The codified chord stress function (Q_f) was adopted for all design methods and the material factor (C_f) equals 1.0 for all the joints.

Table 7

Evaluation of design methods, without using the C_f factor, against test results of 46 screened RHS-to-RHS X joints under brace axial compression.

Specimen	f_{y0} (MPa)	θ_1 (°)	n	η*	N_{1u} (kN)	$N_{1u}/N_{C,M}$	N_{1u}/N_{Yu}	N_{1u}/N_{Kuhn}	N_{1u}/N_{Lan}	$N_{1u}/N_{P,M}$	$N_{1u}/N_{P,LK}$
X(4)RR45	320	45	0	1.00	372	1.24	1.16	1.25	1.04	1.24	1.25
X-RR-90-A	432	90	0	1.00	391	1.09	1.02	1.11	0.92	1.09	1.11
X-RR-60-A	432	60	0	1.00	410	1.06	1.00	1.08	0.90	1.06	1.08
X-RR-45-A	432	45	0	1.00	450	1.05	0.99	1.07	0.89	1.05	1.07
X-RR-90-C	237	90	0	1.00	680	1.06	0.97	1.06	0.88	1.06	1.05
X-RR-60-C	237	60	0	1.00	672	0.97	0.89	0.97	0.81	0.97	0.97
X-RR-45-C	228	45	0	1.00	846	1.08	0.99	1.08	0.90	1.08	1.08
10P	304	90	0	1.00	276	1.11	1.04	1.12	0.95	1.11	1.13
11P	304	90	-0.43	1.00	271	1.16	1.08	1.16	0.99	1.16	1.17
12P	304	90	-0.87	1.00	275	1.36	1.27	1.36	1.16	1.36	1.37
13P	304	90	-0.87	1.00	280	1.38	1.29	1.39	1.18	1.38	1.40
14P	304	90	-0.65	1.00	271	1.21	1.14	1.22	1.04	1.21	1.23
15P	304	90	-0.22	1.00	263	1.09	1.02	1.09	0.93	1.09	1.10
5B	336	90	-0.71	1.00	313	1.22	1.14	1.23	1.04	1.22	1.23
6B	336	90	-0.76	1.00	284	1.17	1.09	1.18	0.99	1.17	1.18
PWLR	388	90	0	1.00	438	1.19	1.16	1.25	1.06	1.19	1.14
DD1122	370	90	0	1.00	445	1.09	1.07	1.10	0.96	1.09	1.11
DD1222	370	45	0	1.00	476	0.99	0.96	0.99	0.87	0.99	1.00
DD1322	370	60	0	1.00	459	1.05	1.03	1.06	0.93	1.05	1.07
DD2121	406	90	0	1.00	1315	1.23	1.09	1.24	1.03	1.23	1.24
DD2122	406	90	0	1.00	1230	1.11	1.06	1.10	0.92	1.11	1.07
DD2222	406	45	0	1.00	1675	1.27	1.21	1.26	1.06	1.27	1.22
DD3121	392	90	0	1.00	649	1.34	1.21	1.35	1.13	1.34	1.34
DD3122	412	90	0	1.00	530	1.06	1.00	1.05	0.88	1.06	1.02
DD3221	392	44	0	1.00	693	1.19	1.07	1.21	1.00	1.19	1.19
DD3222	412	44	0	1.00	694	1.16	1.09	1.15	0.96	1.16	1.11
DD4123	406	90	0	1.00	2183	1.23	1.14	1.24	1.03	1.23	1.24
DD4223	406	45	0	1.00	2429	1.15	1.07	1.16	0.97	1.15	1.16
DD4323	406	60	0	1.00	2215	1.16	1.08	1.17	0.98	1.16	1.17
X1	330	90	0	1.00	176	1.10	1.02	1.11	0.92	1.10	1.10
X2	330	90	0	1.00	302	1.20	1.12	1.22	1.01	1.20	1.22
X3	400	90	0	1.00	373	0.88	0.83	0.89	0.77	0.88	0.89
X4	370	90	0	1.00	560	1.10	1.06	1.10	1.01	1.10	1.11
X5	345	90	0	1.00	783	1.05	1.05	1.04	1.03	1.05	1.06
X6	463	90	0	0.60	409	1.22	1.13	1.25	0.83	1.13	1.07
X7	451	90	0	1.00	828	1.11	1.04	1.13	0.94	1.11	1.13
X9	481	90	0	0.75	1289	1.25	1.15	1.31	0.94	1.20	1.15
X-100×50×4-100×50×4	952	90	0	1.00	482	1.01	0.90	1.03	0.91	1.01	1.04
X-120×120×4-120×120×4	971	90	0	1.00	567	1.07	0.99	1.10	0.92	1.07	1.04
X-140×140×4-140×140×4	1008	90	0	0.99	484	0.94	0.87	1.02	0.86	0.94	0.93
X-120×120×3-120×120×3	1038	90	0	1.00	317	1.05	0.97	1.26	1.08	1.05	1.10
X-80×80×4-80×80×4	1004	90	0	1.00	595	1.02	0.97	1.05	0.88	1.02	1.04
X-120×120×4-120×120×3	1038	90	0	1.00	318	1.07	0.99	1.31	1.13	1.07	1.13
X5-S500	548	90	0	1.00	815	1.20	1.11	1.21	1.01	1.20	1.20
X5-S700	762	90	0	1.00	935	1.17	1.09	1.19	1.00	1.17	1.16
X5-S960	1080	90	0	1.00	808	0.90	0.84	0.93	0.79	0.90	0.88
Mean						1.13	1.05	1.15	0.97	1.12	1.13
CoV						0.098	0.096	0.098	0.097	0.097	0.097

Note: The approach of only including a term of $(1/\sin\theta_1)^{0.5}$ in the final resistance equation was adopted for all design methods.

Table 8

Evaluation of design methods, using the C_f factor, against test results of 46 screened RHS-to-RHS X joints under brace axial compression.

Specimen	f_{y0} (MPa)	θ_1 (°)	n	η^*	N_{1u} (kN)	$N_{1u}/N_{C,M}$	N_{1u}/N_{Yu}	N_{1u}/N_{Kuhn}	N_{1u}/N_{Lan}	$N_{1u}/N_{P,M}$	$N_{1u}/N_{P,LK}$
X(4)RR45	320	45	0	1.00	372	1.24	1.16	1.25	1.04	1.24	1.25
X-RR-90-A	432	90	0	1.00	391	1.11	1.05	1.13	0.94	1.11	1.13
X-RR-60-A	432	60	0	1.00	410	1.09	1.02	1.10	0.92	1.09	1.10
X-RR-45-A	432	45	0	1.00	450	1.08	1.01	1.09	0.91	1.08	1.09
X-RR-90-C	237	90	0	1.00	680	1.06	0.97	1.06	0.88	1.06	1.05
X-RR-60-C	237	60	0	1.00	672	0.97	0.89	0.97	0.81	0.97	0.97
X-RR-45-C	228	45	0	1.00	846	1.08	0.99	1.08	0.90	1.08	1.08
10P	304	90	0	1.00	276	1.11	1.04	1.12	0.95	1.11	1.13
11P	304	90	-0.43	1.00	271	1.16	1.08	1.16	0.99	1.16	1.17
12P	304	90	-0.87	1.00	275	1.36	1.27	1.36	1.16	1.36	1.37
13P	304	90	-0.87	1.00	280	1.38	1.29	1.39	1.18	1.38	1.40
14P	304	90	-0.65	1.00	271	1.21	1.14	1.22	1.04	1.21	1.23
15P	304	90	-0.22	1.00	263	1.09	1.02	1.09	0.93	1.09	1.10
5B	336	90	-0.71	1.00	313	1.22	1.14	1.23	1.04	1.22	1.23
6B	336	90	-0.76	1.00	284	1.17	1.09	1.18	0.99	1.17	1.18
PWLR	388	90	0	1.00	438	1.20	1.17	1.26	1.07	1.20	1.15
DD1122	370	90	0	1.00	445	1.10	1.07	1.11	0.97	1.10	1.12
DD1222	370	45	0	1.00	476	0.99	0.97	1.00	0.87	0.99	1.00
DD1322	370	60	0	1.00	459	1.06	1.03	1.06	0.93	1.06	1.07
DD2121	406	90	0	1.00	1315	1.24	1.10	1.26	1.05	1.24	1.25
DD2122	406	90	0	1.00	1230	1.13	1.07	1.12	0.94	1.13	1.08
DD2222	406	45	0	1.00	1675	1.29	1.23	1.28	1.07	1.29	1.24
DD3121	392	90	0	1.00	649	1.36	1.22	1.37	1.14	1.36	1.36
DD3122	412	90	0	1.00	530	1.08	1.01	1.07	0.90	1.08	1.03
DD3221	392	44	0	1.00	693	1.21	1.08	1.22	1.01	1.21	1.21
DD3222	412	44	0	1.00	694	1.18	1.11	1.17	0.98	1.18	1.13
DD4123	406	90	0	1.00	2183	1.24	1.16	1.26	1.05	1.24	1.26
DD4223	406	45	0	1.00	2429	1.16	1.08	1.18	0.98	1.16	1.18
DD4323	406	60	0	1.00	2215	1.18	1.09	1.19	0.99	1.18	1.19
X1	330	90	0	1.00	176	1.10	1.02	1.11	0.92	1.10	1.10
X2	330	90	0	1.00	302	1.20	1.12	1.22	1.01	1.20	1.22
X3	400	90	0	1.00	373	0.89	0.84	0.90	0.78	0.89	0.90
X4	370	90	0	1.00	560	1.10	1.06	1.11	1.02	1.10	1.12
X5	345	90	0	1.00	783	1.05	1.05	1.04	1.03	1.05	1.06
X6	463	90	0	0.60	409	1.26	1.16	1.29	0.86	1.16	1.11
X7	451	90	0	1.00	828	1.14	1.07	1.16	0.97	1.14	1.16
X9	481	90	0	0.75	1289	1.30	1.19	1.36	0.98	1.24	1.19
X-100×50×4-100×50×4	952	90	0	1.00	482	1.21	1.08	1.24	1.09	1.21	1.25
X-120×120×4-120×120×4	971	90	0	1.00	567	1.29	1.20	1.32	1.11	1.29	1.26
X-140×140×4-140×140×4	1008	90	0	0.99	484	1.15	1.06	1.25	1.05	1.15	1.14
X-120×120×3-120×120×3	1038	90	0	1.00	317	1.30	1.20	1.56	1.33	1.30	1.36
X-80×80×4-80×80×4	1004	90	0	1.00	595	1.25	1.18	1.29	1.07	1.25	1.28
X-120×120×4-120×120×3	1038	90	0	1.00	318	1.33	1.22	1.62	1.40	1.33	1.41
X5-S500	548	90	0	1.00	815	1.27	1.18	1.28	1.07	1.27	1.27
X5-S700	762	90	0	1.00	935	1.33	1.23	1.34	1.12	1.33	1.30
X5-S960	1080	90	0	1.00	808	1.13	1.05	1.17	0.99	1.13	1.11
Mean						1.17	1.10	1.20	1.01	1.17	1.17
CoV						0.092	0.086	0.116	0.116	0.091	0.095

Note: The approach of only including a term of $(1/\sin\theta_1)^{0.5}$ in the final resistance equation was adopted for all design methods.

Table 9

Collated numerical results totalling 173 RHS-to-RHS X joints under brace axial compression.

Researcher/year	Specimen	b_0 (mm)	h_0 (mm)	t_0 (mm)	b_1 (mm)	h_1 (mm)	t_1 (mm)	f_{y0} (MPa)	θ_1 (°)	n	η*	2γ*	N_{1u} (kN)	N_{1u}/N_y
Yu/1997	x10ae05	150	150	10.00	150	75	10.00	355	90	0	0.50	15	1019	1.15
	x10ae	150	150	10.00	150	150	10.00	355	90	0	1.00	15	1507	1.06
	x10ae2	150	150	10.00	150	300	10.00	355	90	0	2.00	15	2498	1.01
	x11ae05	150	150	6.25	150	75	6.25	355	90	0	0.50	24	509	1.08
	x11a	150	150	6.25	150	150	6.25	355	90	0	1.00	24	776	0.96
	x11ae2	150	150	6.25	150	300	6.25	355	90	0	2.00	24	1427	0.97
	x12ae05	150	150	4.29	150	75	4.29	355	90	0	0.50	35	302	1.03
	x12ae	150	150	4.29	150	150	4.29	355	90	0	1.00	35	482	0.92
	x12ae2	150	150	4.29	150	300	4.29	355	90	0	2.00	35	816	0.83
	x10a-0	150	150	10.00	150	150	10.00	355	90	0	1.00	15	1611	1.13
	x10a-0.4	150	150	10.00	150	150	10.00	355	90	-0.40	1.00	15	1587	1.12
	x10a-0.6	150	150	10.00	150	150	10.00	355	90	-0.60	1.00	15	1562	1.10
	x10a-0.8	150	150	10.00	150	150	10.00	355	90	-0.80	1.00	15	1492	1.05
	x11a-0	150	150	6.25	150	150	6.25	355	90	0	1.00	24	817	1.02
	x11a-0.4	150	150	6.25	150	150	6.25	355	90	-0.40	1.00	24	803	1.00
	x11a-0.6	150	150	6.25	150	150	6.25	355	90	-0.60	1.00	24	787	0.98
	x11a-0.8	150	150	6.25	150	150	6.25	355	90	-0.80	1.00	24	757	0.94
	x12a-0	150	150	4.29	150	150	4.29	355	90	0	1.00	35	502	0.96
	x12a-0.4	150	150	4.29	150	150	4.29	355	90	-0.40	1.00	35	498	0.95
	x12a-0.6	150	150	4.29	150	150	4.29	355	90	-0.60	1.00	35	484	0.93
	x12a-0.8	150	150	4.29	150	150	4.29	355	90	-0.80	1.00	35	459	0.88
Kuhn/2019	Para_1	200	80	8.00	200	400	11.00	398	90	0	5.00	10	3239	1.16
	Para_26	200	80	8.00	200	400	11.00	398	90	-0.25	5.00	10	3252	1.16
	Para_51	200	80	8.00	200	400	11.00	398	90	-0.50	5.00	10	3252	1.16
	Para_76	200	80	8.00	200	400	11.00	398	90	-0.75	5.00	10	3237	1.15
	Para_101	200	80	8.00	200	400	11.00	398	90	0.25	5.00	10	3225	1.15
	Para_126	200	80	8.00	200	400	11.00	398	90	0.50	5.00	10	3186	1.14
	Para_151	200	80	8.00	200	400	11.00	398	90	0.75	5.00	10	3135	1.12
	Para_2	200	160	8.00	200	400	11.00	398	90	0	2.50	20	2641	0.94
	Para_27	200	160	8.00	200	400	11.00	398	90	-0.25	2.50	20	2676	0.95
	Para_52	200	160	8.00	200	400	11.00	398	90	-0.50	2.50	20	2687	0.96
	Para_77	200	160	8.00	200	400	11.00	398	90	-0.75	2.50	20	2673	0.95
	Para_102	200	160	8.00	200	400	11.00	398	90	0.25	2.50	20	2608	0.93
	Para_127	200	160	8.00	200	400	11.00	398	90	0.50	2.50	20	2530	0.90
	Para_152	200	160	8.00	200	400	11.00	398	90	0.75	2.50	20	2392	0.85
	Para_6	200	80	8.00	200	200	11.00	398	90	0	2.50	10	1742	1.14
	Para_31	200	80	8.00	200	200	11.00	398	90	-0.25	2.50	10	1747	1.14
	Para_56	200	80	8.00	200	200	11.00	398	90	-0.50	2.50	10	1747	1.14
	Para_106	200	80	8.00	200	200	11.00	398	90	0.25	2.50	10	1737	1.14
	Para_131	200	80	8.00	200	200	11.00	398	90	0.50	2.50	10	1720	1.13
	Para_156	200	80	8.00	200	200	11.00	398	90	0.75	2.50	10	1694	1.11
	P_1	80	80	8.00	80	160	11.00	398	90	0	2.00	10	1423	1.12
	P_26	80	80	8.00	80	160	11.00	398	90	-0.25	2.00	10	1434	1.13
	P_51	80	80	8.00	80	160	11.00	398	90	-0.50	2.00	10	1433	1.12
	P_76	80	80	8.00	80	160	11.00	398	90	-0.75	2.00	10	1422	1.12
	P_101	80	80	8.00	80	160	11.00	398	90	0.25	2.00	10	1401	1.10
	P_126	80	80	8.00	80	160	11.00	398	90	0.50	2.00	10	1360	1.07
	P_151	80	80	8.00	80	160	11.00	398	90	0.75	2.00	10	1292	1.01
	P_2	160	160	8.00	160	320	11.00	398	90	0	2.00	20	2201	0.96
	P_27	160	160	8.00	160	320	11.00	398	90	-0.25	2.00	20	2228	0.97
	P_52	160	160	8.00	160	320	11.00	398	90	-0.50	2.00	20	2237	0.98
	P_77	160	160	8.00	160	320	11.00	398	90	-0.75	2.00	20	2237	0.98
	P_102	160	160	8.00	160	320	11.00	398	90	0.25	2.00	20	2170	0.95
	P_127	160	160	8.00	160	320	11.00	398	90	0.50	2.00	20	2088	0.91
	P_152	160	160	8.00	160	320	11.00	398	90	0.75	2.00	20	1969	0.86
	P_3	240	240	8.00	240	480	11.00	398	90	0	2.00	30	2504	0.76
	P_28	240	240	8.00	240	480	11.00	398	90	-0.25	2.00	30	2549	0.77
	P_53	240	240	8.00	240	480	11.00	398	90	-0.50	2.00	30	2561	0.77

P_78	240	240	8.00	240	480	11.00	398	90	-0.75	2.00	30	2532	0.76
P_103	240	240	8.00	240	480	11.00	398	90	0.25	2.00	30	2465	0.74
P_128	240	240	8.00	240	480	11.00	398	90	0.50	2.00	30	2408	0.73
P_153	240	240	8.00	240	480	11.00	398	90	0.75	2.00	30	2257	0.68
Para_3	200	240	8.00	200	400	11.00	398	90	0	1.67	30	2198	0.78
Para_28	200	240	8.00	200	400	11.00	398	90	-0.25	1.67	30	2235	0.80
Para_53	200	240	8.00	200	400	11.00	398	90	-0.50	1.67	30	2236	0.80
Para_78	200	240	8.00	200	400	11.00	398	90	-0.75	1.67	30	2217	0.79
Para_103	200	240	8.00	200	400	11.00	398	90	0.25	1.67	30	2166	0.77
Para_128	200	240	8.00	200	400	11.00	398	90	0.50	1.67	30	2112	0.75
Para_153	200	240	8.00	200	400	11.00	398	90	0.75	1.67	30	1967	0.70
Para_7	200	160	8.00	200	200	11.00	398	90	0	1.25	20	1511	0.99
Para_32	200	160	8.00	200	200	11.00	398	90	-0.25	1.25	20	1526	1.00
Para_57	200	160	8.00	200	200	11.00	398	90	-0.50	1.25	20	1516	0.99
Para_82	200	160	8.00	200	200	11.00	398	90	-0.75	1.25	20	1502	0.98
Para_107	200	160	8.00	200	200	11.00	398	90	0.25	1.25	20	1498	0.98
Para_132	200	160	8.00	200	200	11.00	398	90	0.50	1.25	20	1456	0.95
Para_157	200	160	8.00	200	200	11.00	398	90	0.75	1.25	20	1384	0.91
Para_11	200	80	8.00	200	100	11.00	398	90	0	1.25	10	987	1.11
Para_36	200	80	8.00	200	100	11.00	398	90	-0.25	1.25	10	984	1.10
Para_61	200	80	8.00	200	100	11.00	398	90	-0.50	1.25	10	974	1.09
Para_86	200	80	8.00	200	100	11.00	398	90	-0.75	1.25	10	957	1.07
Para_111	200	80	8.00	200	100	11.00	398	90	0.25	1.25	10	990	1.11
Para_136	200	80	8.00	200	100	11.00	398	90	0.50	1.25	10	987	1.11
Para_161	200	80	8.00	200	100	11.00	398	90	0.75	1.25	10	975	1.09
P_6	80	80	8.00	80	80	11.00	398	90	0	1.00	10	823	1.08
P_31	80	80	8.00	80	80	11.00	398	90	-0.25	1.00	10	826	1.08
P_56	80	80	8.00	80	80	11.00	398	90	-0.50	1.00	10	817	1.07
P_81	80	80	8.00	80	80	11.00	398	90	-0.75	1.00	10	795	1.04
P_106	80	80	8.00	80	80	11.00	398	90	0.25	1.00	10	810	1.06
P_131	80	80	8.00	80	80	11.00	398	90	0.50	1.00	10	775	1.01
P_156	80	80	8.00	80	80	11.00	398	90	0.75	1.00	10	706	0.92
P_7	160	160	8.00	160	160	11.00	398	90	0	1.00	20	1279	1.00
P_32	160	160	8.00	160	160	11.00	398	90	-0.25	1.00	20	1287	1.01
P_57	160	160	8.00	160	160	11.00	398	90	-0.50	1.00	20	1274	1.00
P_82	160	160	8.00	160	160	11.00	398	90	-0.75	1.00	20	1250	0.98
P_107	160	160	8.00	160	160	11.00	398	90	0.25	1.00	20	1266	0.99
P_132	160	160	8.00	160	160	11.00	398	90	0.50	1.00	20	1223	0.96
P_157	160	160	8.00	160	160	11.00	398	90	0.75	1.00	20	1145	0.90
P_8	240	240	8.00	240	240	11.00	398	90	0	1.00	30	1547	0.87
P_33	240	240	8.00	240	240	11.00	398	90	-0.25	1.00	30	1547	0.87
P_58	240	240	8.00	240	240	11.00	398	90	-0.50	1.00	30	1530	0.86
P_83	240	240	8.00	240	240	11.00	398	90	-0.75	1.00	30	1490	0.84
P_108	240	240	8.00	240	240	11.00	398	90	0.25	1.00	30	1551	0.87
P_133	240	240	8.00	240	240	11.00	398	90	0.50	1.00	30	1507	0.84
P_158	240	240	8.00	240	240	11.00	398	90	0.75	1.00	30	1418	0.80
Para_8	200	240	8.00	200	200	11.00	398	90	0	0.83	30	1385	0.91
Para_33	200	240	8.00	200	200	11.00	398	90	-0.25	0.83	30	1380	0.90
Para_58	200	240	8.00	200	200	11.00	398	90	-0.50	0.83	30	1352	0.88
Para_83	200	240	8.00	200	200	11.00	398	90	-0.75	0.83	30	1302	0.85
Para_108	200	240	8.00	200	200	11.00	398	90	0.25	0.83	30	1385	0.91
Para_133	200	240	8.00	200	200	11.00	398	90	0.50	0.83	30	1340	0.88
Para_158	200	240	8.00	200	200	11.00	398	90	0.75	0.83	30	1246	0.82
Para_12	200	160	8.00	200	100	11.00	398	90	0	0.63	20	933	1.05
Para_37	200	160	8.00	200	100	11.00	398	90	-0.25	0.63	20	936	1.05
Para_62	200	160	8.00	200	100	11.00	398	90	-0.50	0.63	20	918	1.03
Para_87	200	160	8.00	200	100	11.00	398	90	-0.75	0.63	20	881	0.99
Para_112	200	160	8.00	200	100	11.00	398	90	0.25	0.63	20	930	1.04
Para_137	200	160	8.00	200	100	11.00	398	90	0.50	0.63	20	908	1.02
Para_162	200	160	8.00	200	100	11.00	398	90	0.75	0.63	20	863	0.97
Para_16	200	80	8.00	200	50	11.00	398	90	0	0.63	10	626	1.09
Para_41	200	80	8.00	200	50	11.00	398	90	-0.25	0.63	10	618	1.08
Para_66	200	80	8.00	200	50	11.00	398	90	-0.50	0.63	10	603	1.05

Para_91	200	80	8.00	200	50	11.00	398	90	-0.75	0.63	10	581	1.01
Para_116	200	80	8.00	200	50	11.00	398	90	0.25	0.63	10	632	1.10
Para_141	200	80	8.00	200	50	11.00	398	90	0.50	0.63	10	633	1.10
Para_166	200	80	8.00	200	50	11.00	398	90	0.75	0.63	10	629	1.10
P_11	80	80	8.00	80	40	11.00	398	90	0	0.50	10	596	1.17
P_36	80	80	8.00	80	40	11.00	398	90	-0.25	0.50	10	596	1.17
P_61	80	80	8.00	80	40	11.00	398	90	-0.50	0.50	10	585	1.15
P_86	80	80	8.00	80	40	11.00	398	90	-0.75	0.50	10	558	1.10
P_111	80	80	8.00	80	40	11.00	398	90	0.25	0.50	10	576	1.13
P_136	80	80	8.00	80	40	11.00	398	90	0.50	0.50	10	540	1.06
P_161	80	80	8.00	80	40	11.00	398	90	0.75	0.50	10	476	0.93
P_12	160	160	8.00	160	80	11.00	398	90	0	0.50	20	824	1.08
P_37	160	160	8.00	160	80	11.00	398	90	-0.25	0.50	20	822	1.08
P_62	160	160	8.00	160	80	11.00	398	90	-0.50	0.50	20	800	1.05
P_87	160	160	8.00	160	80	11.00	398	90	-0.75	0.50	20	758	0.99
P_112	160	160	8.00	160	80	11.00	398	90	0.25	0.50	20	820	1.07
P_137	160	160	8.00	160	80	11.00	398	90	0.50	0.50	20	799	1.05
P_162	160	160	8.00	160	80	11.00	398	90	0.75	0.50	20	749	0.98
P_13	240	240	8.00	240	120	11.00	398	90	0	0.50	30	1039	1.02
P_38	240	240	8.00	240	120	11.00	398	90	-0.25	0.50	30	1025	1.01
P_63	240	240	8.00	240	120	11.00	398	90	-0.50	0.50	30	984	0.97
P_88	240	240	8.00	240	120	11.00	398	90	-0.75	0.50	30	914	0.90
P_138	240	240	8.00	240	120	11.00	398	90	0.50	0.50	30	1020	1.00
P_163	240	240	8.00	240	120	11.00	398	90	0.75	0.50	30	964	0.95
Para_13	200	240	8.00	200	100	11.00	398	90	0	0.42	30	949	1.06
Para_38	200	240	8.00	200	100	11.00	398	90	-0.25	0.42	30	936	1.05
Para_63	200	240	8.00	200	100	11.00	398	90	-0.50	0.42	30	892	1.00
Para_88	200	240	8.00	200	100	11.00	398	90	-0.75	0.42	30	816	0.91
Para_113	200	240	8.00	200	100	11.00	398	90	0.25	0.42	30	958	1.07
Para_138	200	240	8.00	200	100	11.00	398	90	0.50	0.42	30	935	1.05
Para_163	200	240	8.00	200	100	11.00	398	90	0.75	0.42	30	878	0.98
Para_17	200	160	8.00	200	50	11.00	398	90	0	0.31	20	651	1.14
Para_42	200	160	8.00	200	50	11.00	398	90	-0.25	0.31	20	637	1.11
Para_67	200	160	8.00	200	50	11.00	398	90	-0.50	0.31	20	610	1.06
Para_92	200	160	8.00	200	50	11.00	398	90	-0.75	0.31	20	569	0.99
Para_117	200	160	8.00	200	50	11.00	398	90	0.25	0.31	20	661	1.15
Para_142	200	160	8.00	200	50	11.00	398	90	0.50	0.31	20	661	1.15
Para_18	200	240	8.00	200	50	11.00	398	90	0	0.21	30	662	1.15
Para_43	200	240	8.00	200	50	11.00	398	90	-0.25	0.21	30	646	1.13
Para_68	200	240	8.00	200	50	11.00	398	90	-0.50	0.21	30	609	1.06
Para_93	200	240	8.00	200	50	11.00	398	90	-0.75	0.21	30	551	0.96
Para_118	200	240	8.00	200	50	11.00	398	90	0.25	0.21	30	687	1.20
Para_143	200	240	8.00	200	50	11.00	398	90	0.50	0.21	30	693	1.21
Para_168	200	240	8.00	200	50	11.00	398	90	0.75	0.21	30	677	1.18
Para_167	200	160	8.00	200	50	11.00	398	90	0.75	0.31	20	643	1.12
P_18	240	240	8.00	240	60	11.00	398	90	0	0.25	30	730	1.15
P_43	240	240	8.00	240	60	11.00	398	90	-0.25	0.25	30	712	1.12
P_68	240	240	8.00	240	60	11.00	398	90	-0.50	0.25	30	676	1.06
P_93	240	240	8.00	240	60	11.00	398	90	-0.75	0.25	30	613	0.96
P_118	240	240	8.00	240	60	11.00	398	90	0.25	0.25	30	746	1.17
P_143	240	240	8.00	240	60	11.00	398	90	0.50	0.25	30	753	1.18
P_168	240	240	8.00	240	60	11.00	398	90	0.75	0.25	30	743	1.17

Table 10

Numerical results of 22 RHS-to-RHS X joints selected to examine the effect of η^* ratio.

Specimen	f_{y0} (MPa)	θ_1 (°)	n	η^*	N_{1u} (kN)	$N_{1u}/N_{C,M}$	N_{1u}/N_{Yu}	N_{1u}/N_{Kuhn}	N_{1u}/N_{Lan}	$N_{1u}/N_{P,M}$	$N_{1u}/N_{P,LK}$
x10ae	355	90	0	1.00	1019	1.11	1.09	1.11	1.06	1.11	1.13
x10ae2	355	90	0	2.00	1507	1.06	1.04	1.05	1.01	1.17	1.19
x11ae05	355	90	0	0.50	2498	1.28	1.15	1.29	1.08	1.15	1.17
x11a	355	90	0	1.00	509	1.14	1.07	1.15	0.96	1.14	1.16
x11ae2	355	90	0	2.00	776	1.15	1.11	1.16	1.06	1.28	1.29
x12ae05	355	90	0	0.50	1427	1.48	1.29	1.49	1.10	1.33	1.32
x12ae	355	90	0	1.00	302	1.33	1.22	1.33	1.11	1.33	1.32
x12ae2	355	90	0	2.00	482	1.20	1.15	1.20	1.19	1.33	1.32
Para_2	398	90	0	2.50	1507	1.08	1.04	1.09	1.01	1.24	1.26
P_2	398	90	0	2.00	2498	1.10	1.07	1.11	1.00	1.22	1.24
P_3	398	90	0	2.00	509	1.03	0.99	1.04	1.00	1.14	1.15
Para_3	398	90	0	1.67	776	1.07	1.03	1.08	1.00	1.16	1.16
Para_7	398	90	0	1.25	1427	1.14	1.06	1.15	1.00	1.18	1.20
P_6	398	90	0	1.00	302	1.09	1.13	1.09	1.09	1.09	1.10
P_7	398	90	0	1.00	482	1.15	1.10	1.16	1.02	1.15	1.17
P_8	398	90	0	1.00	816	1.18	1.10	1.20	1.00	1.18	1.19
Para_8	398	90	0	0.83	2641	1.24	1.16	1.25	1.01	1.20	1.21
Para_12	398	90	0	0.63	2201	1.20	1.08	1.21	1.06	1.12	1.14
Para_16	398	90	0	0.63	2504	1.11	0.93	1.11	1.11	1.11	1.11
P_12	398	90	0	0.50	2198	1.24	1.14	1.25	1.09	1.12	1.14
P_13	398	90	0	0.50	1511	1.39	1.22	1.41	1.06	1.25	1.26
Para_13	398	90	0	0.42	823	1.45	1.30	1.47	1.08	1.27	1.28
Mean						1.19	1.11	1.20	1.05	1.20	1.20
CoV						0.105	0.080	0.106	0.051	0.064	0.059

Note: The material factor (C_f) was used for all the design methods.

Table 11
Numerical results of 10 RHS-to-RHS X joints selected to examine the chord stress effect.

Specimen	f_{y0} (MPa)	θ_1 (°)	n	η*	N_{1u} (kN)	$N_{1u}/N_{C,M}$	N_{1u}/N_{Yu}	N_{1u}/N_{Kuhn}	N_{1u}/N_{Lan}	$N_{1u}/N_{P,M}$	$N_{1u}/N_{P,LK}$
x10a-0.6	355	90	-0.6	1.00	1562	1.27	1.24	1.26	1.21	1.27	1.28
x10a-0.8	355	90	-0.8	1.00	1492	1.30	1.27	1.29	1.23	1.30	1.31
x11a-0	355	90	0	1.00	817	1.20	1.13	1.21	1.02	1.20	1.22
x11a-0.4	355	90	-0.4	1.00	803	1.24	1.17	1.26	1.05	1.24	1.26
x11a-0.6	355	90	-0.6	1.00	787	1.27	1.19	1.28	1.07	1.27	1.29
x11a-0.8	355	90	-0.8	1.00	757	1.31	1.23	1.32	1.11	1.31	1.33
x12a-0	355	90	0	1.00	502	1.38	1.27	1.39	1.16	1.38	1.37
x12a-0.4	355	90	-0.4	1.00	498	1.44	1.33	1.45	1.21	1.44	1.43
x12a-0.6	355	90	-0.6	1.00	484	1.46	1.35	1.47	1.22	1.46	1.45
x12a-0.8	355	90	-0.8	1.00	459	1.48	1.37	1.49	1.24	1.48	1.47
Mean						1.34	1.25	1.34	1.15	1.34	1.34
CoV						0.074	0.063	0.073	0.073	0.074	0.064

Note: The material factor (C_f) equals 1.0 for all the joints.

Table 12

Evaluation of design methods, using the C_f factor, against numerical results of 131 screened RHS-to-RHS X joints under brace axial compression.

Specimen	f_{y0} (MPa)	θ_1 (°)	n	η*	N_{1u} (kN)	$N_{1u}/N_{C,M}$	N_{1u}/N_{Yu}	N_{1u}/N_{Kuhn}	N_{1u}/N_{Lan}	$N_{1u}/N_{P,M}$	$N_{1u}/N_{P,LK}$
x10ae	355	90	0	1.00	1507	1.11	1.09	1.11	1.06	1.11	1.13
x10ae2	355	90	0	2.00	2498	1.06	1.04	1.05	1.01	1.17	1.19
x11ae05	355	90	0	0.50	509	1.28	1.15	1.29	1.08	1.15	1.17
x11a	355	90	0	1.00	776	1.14	1.07	1.15	0.96	1.14	1.16
x11ae2	355	90	0	2.00	1427	1.15	1.11	1.16	1.06	1.28	1.29
x12ae05	355	90	0	0.50	302	1.48	1.29	1.49	1.10	1.33	1.32
x12ae	355	90	0	1.00	482	1.33	1.22	1.33	1.11	1.33	1.32
x12ae2	355	90	0	2.00	816	1.20	1.15	1.20	1.19	1.33	1.32
x10a-0.6	355	90	-0.60	1.00	1562	1.27	1.24	1.26	1.21	1.27	1.28
x10a-0.8	355	90	-0.80	1.00	1492	1.30	1.27	1.29	1.23	1.30	1.31
x11a-0	355	90	0	1.00	817	1.20	1.13	1.21	1.02	1.20	1.22
x11a-0.4	355	90	-0.40	1.00	803	1.24	1.17	1.26	1.05	1.24	1.26
x11a-0.6	355	90	-0.60	1.00	787	1.27	1.19	1.28	1.07	1.27	1.29
x11a-0.8	355	90	-0.80	1.00	757	1.31	1.23	1.32	1.11	1.31	1.33
x12a-0	355	90	0	1.00	502	1.38	1.27	1.39	1.16	1.38	1.37
x12a-0.4	355	90	-0.40	1.00	498	1.44	1.33	1.45	1.21	1.44	1.43
x12a-0.6	355	90	-0.60	1.00	484	1.46	1.35	1.47	1.22	1.46	1.45
x12a-0.8	355	90	-0.80	1.00	459	1.48	1.37	1.49	1.24	1.48	1.47
Para_2	398	90	0	2.50	2641	1.08	1.04	1.09	1.01	1.24	1.26
Para_27	398	90	-0.25	2.50	2676	1.13	1.09	1.14	1.05	1.30	1.32
Para_52	398	90	-0.50	2.50	2687	1.18	1.14	1.19	1.10	1.36	1.38
Para_77	398	90	-0.75	2.50	2673	1.26	1.21	1.27	1.17	1.45	1.47
Para_102	398	90	0.25	2.50	2608	1.10	1.06	1.11	1.03	1.26	1.28
Para_127	398	90	0.50	2.50	2530	1.11	1.07	1.12	1.04	1.28	1.30
Para_152	398	90	0.75	2.50	2392	1.13	1.09	1.14	1.05	1.29	1.31
P_101	398	90	0.25	2.00	1401	1.15	1.17	1.15	1.15	1.27	1.28
P_126	398	90	0.50	2.00	1360	1.16	1.18	1.16	1.16	1.29	1.29
P_151	398	90	0.75	2.00	1292	1.18	1.21	1.18	1.18	1.31	1.32
P_2	398	90	0	2.00	2201	1.10	1.07	1.11	1.00	1.22	1.24
P_27	398	90	-0.25	2.00	2228	1.15	1.12	1.16	1.04	1.28	1.30
P_52	398	90	-0.50	2.00	2237	1.20	1.17	1.21	1.09	1.33	1.36
P_77	398	90	-0.75	2.00	2237	1.29	1.25	1.30	1.17	1.43	1.45
P_102	398	90	0.25	2.00	2170	1.12	1.09	1.13	1.01	1.24	1.26
P_127	398	90	0.50	2.00	2088	1.12	1.09	1.13	1.02	1.25	1.27
P_152	398	90	0.75	2.00	1969	1.13	1.10	1.14	1.03	1.26	1.28
P_3	398	90	0	2.00	2504	1.03	0.99	1.04	1.00	1.14	1.15
P_28	398	90	-0.25	2.00	2549	1.08	1.04	1.09	1.05	1.20	1.20
P_53	398	90	-0.50	2.00	2561	1.13	1.08	1.14	1.10	1.25	1.26
P_78	398	90	-0.75	2.00	2532	1.20	1.15	1.21	1.16	1.33	1.33
P_103	398	90	0.25	2.00	2465	1.04	1.00	1.06	1.01	1.16	1.16
P_128	398	90	0.50	2.00	2408	1.06	1.02	1.07	1.03	1.18	1.18
P_153	398	90	0.75	2.00	2257	1.07	1.02	1.08	1.04	1.18	1.19
Para_3	398	90	0	1.67	2198	1.07	1.03	1.08	1.00	1.16	1.16
Para_28	398	90	-0.25	1.67	2235	1.12	1.08	1.13	1.04	1.21	1.21
Para_53	398	90	-0.50	1.67	2236	1.17	1.12	1.18	1.09	1.26	1.26
Para_78	398	90	-0.75	1.67	2217	1.24	1.19	1.25	1.15	1.34	1.34
Para_103	398	90	0.25	1.67	2166	1.09	1.05	1.10	1.01	1.17	1.18
Para_128	398	90	0.50	1.67	2112	1.10	1.06	1.11	1.02	1.19	1.19
Para_153	398	90	0.75	1.67	1967	1.10	1.06	1.11	1.02	1.19	1.19
Para_7	398	90	0	1.25	1511	1.14	1.06	1.15	1.00	1.18	1.20
Para_32	398	90	-0.25	1.25	1526	1.18	1.10	1.19	1.04	1.22	1.24
Para_57	398	90	-0.50	1.25	1516	1.22	1.14	1.23	1.08	1.26	1.29
Para_82	398	90	-0.75	1.25	1502	1.30	1.21	1.31	1.14	1.34	1.36
Para_107	398	90	0.25	1.25	1498	1.16	1.09	1.17	1.02	1.20	1.22
Para_132	398	90	0.50	1.25	1456	1.17	1.10	1.18	1.03	1.21	1.23
Para_157	398	90	0.75	1.25	1384	1.20	1.12	1.21	1.05	1.24	1.26
Para_36	398	90	-0.25	1.25	984	1.15	1.03	1.15	1.15	1.19	1.20
Para_61	398	90	-0.50	1.25	974	1.19	1.06	1.19	1.19	1.23	1.23

Para_86	398	90	-0.75	1.25	957	1.25	1.12	1.25	1.25	1.29	1.30
Para_161	398	90	0.75	1.25	975	1.27	1.14	1.27	1.27	1.31	1.32
P_6	398	90	0	1.00	823	1.09	1.13	1.09	1.09	1.09	1.10
P_31	398	90	-0.25	1.00	826	1.13	1.17	1.13	1.13	1.13	1.13
P_56	398	90	-0.50	1.00	817	1.16	1.20	1.16	1.16	1.16	1.17
P_81	398	90	-0.75	1.00	795	1.21	1.25	1.21	1.21	1.21	1.22
P_106	398	90	0.25	1.00	810	1.10	1.14	1.10	1.10	1.10	1.11
P_131	398	90	0.50	1.00	775	1.10	1.14	1.10	1.10	1.10	1.11
P_156	398	90	0.75	1.00	706	1.07	1.11	1.07	1.07	1.07	1.08
P_7	398	90	0	1.00	1279	1.15	1.10	1.16	1.02	1.15	1.17
P_32	398	90	-0.25	1.00	1287	1.20	1.14	1.21	1.05	1.20	1.22
P_57	398	90	-0.50	1.00	1274	1.23	1.17	1.24	1.09	1.23	1.25
P_82	398	90	-0.75	1.00	1250	1.30	1.23	1.31	1.14	1.30	1.32
P_107	398	90	0.25	1.00	1266	1.18	1.12	1.19	1.03	1.18	1.20
P_132	398	90	0.50	1.00	1223	1.18	1.12	1.19	1.04	1.18	1.20
P_157	398	90	0.75	1.00	1145	1.19	1.13	1.20	1.04	1.19	1.21
P_8	398	90	0	1.00	1547	1.18	1.10	1.20	1.00	1.18	1.19
P_33	398	90	-0.25	1.00	1547	1.22	1.13	1.23	1.03	1.22	1.22
P_58	398	90	-0.50	1.00	1530	1.25	1.16	1.27	1.06	1.25	1.26
P_83	398	90	-0.75	1.00	1490	1.31	1.21	1.32	1.10	1.31	1.31
P_108	398	90	0.25	1.00	1551	1.22	1.13	1.23	1.03	1.22	1.23
P_133	398	90	0.50	1.00	1507	1.24	1.15	1.25	1.04	1.24	1.24
P_158	398	90	0.75	1.00	1418	1.25	1.16	1.26	1.05	1.25	1.25
Para_8	398	90	0	0.83	1385	1.24	1.16	1.25	1.01	1.20	1.21
Para_33	398	90	-0.25	0.83	1380	1.27	1.19	1.28	1.03	1.23	1.24
Para_58	398	90	-0.50	0.83	1352	1.29	1.21	1.31	1.06	1.26	1.26
Para_83	398	90	-0.75	0.83	1302	1.33	1.25	1.35	1.09	1.30	1.30
Para_108	398	90	0.25	0.83	1385	1.27	1.19	1.29	1.04	1.24	1.24
Para_133	398	90	0.50	0.83	1340	1.28	1.20	1.30	1.05	1.25	1.25
Para_158	398	90	0.75	0.83	1246	1.28	1.19	1.29	1.04	1.24	1.25
Para_12	398	90	0	0.63	933	1.20	1.08	1.21	1.06	1.12	1.14
Para_37	398	90	-0.25	0.63	936	1.24	1.11	1.25	1.09	1.16	1.18
Para_62	398	90	-0.50	0.63	918	1.27	1.13	1.28	1.12	1.18	1.20
Para_87	398	90	-0.75	0.63	881	1.30	1.17	1.32	1.15	1.22	1.24
Para_112	398	90	0.25	0.63	930	1.23	1.10	1.25	1.09	1.15	1.17
Para_137	398	90	0.50	0.63	908	1.25	1.12	1.27	1.10	1.17	1.19
Para_162	398	90	0.75	0.63	863	1.28	1.14	1.29	1.12	1.19	1.21
Para_16	398	90	0	0.63	626	1.11	0.93	1.11	1.11	1.11	1.11
Para_41	398	90	-0.25	0.63	618	1.12	0.95	1.12	1.12	1.12	1.12
Para_66	398	90	-0.50	0.63	603	1.14	0.96	1.14	1.14	1.14	1.14
Para_91	398	90	-0.75	0.63	581	1.18	0.99	1.18	1.18	1.18	1.18
Para_116	398	90	0.25	0.63	632	1.15	0.97	1.15	1.15	1.15	1.15
Para_141	398	90	0.50	0.63	633	1.20	1.01	1.20	1.20	1.20	1.20
Para_166	398	90	0.75	0.63	629	1.27	1.08	1.27	1.27	1.27	1.27
P_86	398	90	-0.75	0.50	558	1.27	1.35	1.27	1.27	1.27	1.27
P_136	398	90	0.50	0.50	540	1.15	1.21	1.15	1.15	1.15	1.15
P_161	398	90	0.75	0.50	476	1.09	1.15	1.09	1.09	1.09	1.09
P_12	398	90	0	0.50	824	1.24	1.14	1.25	1.09	1.12	1.14
P_37	398	90	-0.25	0.50	822	1.27	1.17	1.28	1.12	1.15	1.17
P_62	398	90	-0.50	0.50	800	1.29	1.19	1.30	1.14	1.16	1.18
P_87	398	90	-0.75	0.50	758	1.31	1.20	1.32	1.15	1.18	1.20
P_112	398	90	0.25	0.50	820	1.27	1.17	1.28	1.12	1.14	1.16
P_137	398	90	0.50	0.50	799	1.29	1.18	1.30	1.13	1.16	1.18
P_162	398	90	0.75	0.50	749	1.29	1.19	1.30	1.14	1.17	1.19
P_13	398	90	0	0.50	1039	1.39	1.22	1.41	1.06	1.25	1.26
P_38	398	90	-0.25	0.50	1025	1.41	1.24	1.43	1.07	1.27	1.28
P_63	398	90	-0.50	0.50	984	1.41	1.24	1.43	1.07	1.27	1.28
P_88	398	90	-0.75	0.50	914	1.41	1.24	1.42	1.07	1.27	1.27
P_138	398	90	0.50	0.50	1020	1.46	1.29	1.48	1.11	1.32	1.33
P_163	398	90	0.75	0.50	964	1.48	1.30	1.50	1.13	1.34	1.34
Para_13	398	90	0	0.42	949	1.45	1.30	1.47	1.08	1.27	1.28
Para_38	398	90	-0.25	0.42	936	1.47	1.32	1.49	1.09	1.29	1.30
Para_63	398	90	-0.50	0.42	892	1.46	1.31	1.48	1.09	1.28	1.29

Para_88	398	90	-0.75	0.42	816	1.43	1.28	1.45	1.06	1.26	1.26
Para_113	398	90	0.25	0.42	958	1.51	1.35	1.52	1.12	1.32	1.33
Para_138	398	90	0.50	0.42	935	1.53	1.37	1.55	1.14	1.34	1.35
Para_163	398	90	0.75	0.42	878	1.54	1.38	1.56	1.15	1.35	1.36
Para_67	398	90	-0.50	0.31	610	1.31	1.11	1.32	1.15	1.15	1.15
Para_92	398	90	-0.75	0.31	569	1.31	1.11	1.32	1.15	1.15	1.15
Para_68	398	90	-0.50	0.21	609	1.55	1.31	1.57	1.15	1.23	1.23
Para_93	398	90	-0.75	0.21	551	1.51	1.27	1.52	1.12	1.19	1.20
P_68	398	90	-0.50	0.25	676	1.55	1.27	1.57	1.15	1.26	1.27
P_93	398	90	-0.75	0.25	613	1.51	1.24	1.52	1.12	1.23	1.23
Mean						1.24	1.15	1.25	1.10	1.23	1.24
CoV						0.102	0.082	0.104	0.061	0.065	0.064

Note: The material factor (C_f) was used for all the design methods.

Table 13

Collated test results totalling 24 RHS X joints with only one RHS brace welded to the chord and under brace axial compression.

Researcher/year	Specimen	b_0 (mm)	h_0 (mm)	t_0 (mm)	b_1 (mm)	h_1 (mm)	t_1 (mm)	f_{y0} (MPa)	θ_1 (°)	n	$2\gamma^*$	η^*	N_{1u} (kN)	N_{1u}/N_y
Barentse/1977	T-RR-A-A-1	101.4	101.4	6.23	101.4	70.0	6.23	299	90	0	16.3	0.69	417	1.11
	T-RR-A-A-7	101.3	101.3	4.03	100.2	70.0	3.77	326	90	0	25.1	0.69	210	0.89
	T-RR-A-A-10	100.4	100.4	2.88	100.4	70.0	2.88	299	90	0	34.9	0.70	112	0.77
	T-RR-E-A-91	101.3	50.9	6.27	101.3	50.9	6.27	322	90	0	8.1	1.00	453	1.36
	T-RR-E-A-94	101.8	50.9	4.73	101.6	50.8	4.90	338	90	0	10.8	1.00	298	1.25
	T-RR-E-A-97	101.3	51.0	3.35	101.3	51.0	3.35	293	90	0	15.2	1.00	150	1.13
	T-RR-E-A-112	102.1	151.3	6.23	101.4	70.0	6.18	289	90	0	24.3	0.46	394	1.08
	T-RR-E-A-119	101.2	151.4	4.82	101.4	70.0	6.23	293	90	0	31.4	0.46	256	0.96
	T-RR-E-A-126	80.6	119.7	3.05	80.2	70.0	3.00	398	90	0	39.2	0.58	142	0.69
	T-RR-C-A-46	100.2	100.2	3.77	100.0	25.0	3.08	349	90	0	26.6	0.25	180	1.16
	T-RR-C-A-50	100.8	100.8	3.36	100.0	25.0	3.02	290	90	0	30.0	0.25	152	1.37
	T-RR-C-A-41	101.4	101.4	6.18	100.9	70.0	3.92	298	90	0	16.4	0.69	394	1.06
	T-RR-C-A-45	101.0	101.0	4.00	100.9	70.0	3.92	343	90	0	25.3	0.69	248	1.00
	T-RR-C-A-49	100.8	100.8	3.36	99.8	70.0	4.00	290	90	0	30.0	0.69	163	0.96
Zhao/2000	S1B1C11	51.0	102.0	4.90	51.0	51.0	4.90	409	90	0	20.8	0.50	316	1.04
	S1B1C12	51.0	102.0	3.20	51.0	51.0	4.90	343	90	0	31.9	0.50	163	1.11
	S1B2C21	102.0	102.0	9.50	102.0	102.0	8.00	445	90	0	10.7	1.00	1207	0.95
	S1B2C22	102.0	102.0	6.30	102.0	102.0	8.00	432	90	0	16.2	1.00	652	0.90
Pandey/2019	TF-100x50x4-100x50x4	100.6	50.6	3.96	100.6	50.6	3.97	952	90	0	12.8	1.00	494	0.93
	TF-120x120x4-120x120x4	121.6	121.6	3.91	121.6	121.7	3.91	971	90	0	31.1	1.00	558	0.52
	TF-140x140x4-140x140x4	141.6	140.3	3.97	141.7	140.4	4.00	1008	90	0	35.3	1.00	544	0.42
	TF-120x120x3-120x120x3	120.9	120.3	3.12	120.8	120.3	3.11	1038	90	0	38.5	1.00	369	0.42
Fan/2017	X-1.0-32-700O	203.6	203.6	5.96	204.0	204.0	11.67	404	90	0	34.2	1.00	653	0.58
	X-1.0-21-550O	203.1	203.1	8.85	204.0	204.0	11.67	418	90	0	22.9	1.00	1264	0.69

Table 14

Evaluation of proposed design methods, using the C_f factor, against test results of eight RHS X joints classified as class a.

Specimen	f_{y0} (MPa)	θ_1 (°)	n	η*	N_{1u} (kN)	$N_{1u}/N_{P,M}$	$N_{1u}/N_{P,LK}$
T-RR-A-A-7	326	90	0	0.69	210	1.00	1.01
T-RR-A-A-10	299	90	0	0.70	112	0.99	0.99
T-RR-E-A-112	289	90	0	0.46	394	1.11	1.12
T-RR-E-A-119	293	90	0	0.46	256	1.10	1.10
T-RR-E-A-126	398	90	0	0.58	142	1.06	1.03
T-RR-C-A-41	298	90	0	0.69	394	1.06	1.07
T-RR-C-A-45	343	90	0	0.69	248	1.14	1.16
T-RR-C-A-49	290	90	0	0.69	163	1.14	1.15
Mean						1.07	1.08
CoV						0.054	0.059

Table 15

Evaluation of proposed design methods, using the C_f factor, against test results of six RHS X joints classified as class b.

Specimen	f_{y0} (MPa)	θ_1 (°)	n	2γ*	2γ* limit	η*	N_{1u} (kN)	$N_{1u}/N_{P,M}$	$N_{1u}/N_{P,LK}$
S1B1C11	409	90	0	20.8	37	0.50	316	1.26	1.29
S1B2C21	445	90	0	10.7	36	1.00	1207	1.04	1.07
S1B2C22	432	90	0	16.2	36	1.00	652	1.09	1.12
TF-100x50x4-100x50x4	952	90	0	12.8	24	1.00	494	1.39	1.47
X-1.0-32-700O	404	90	0	34.2	37	1.00	653	1.20	1.18
X-1.0-21-550O	418	90	0	22.9	37	1.00	1264	0.98	1.01
Mean								1.16	1.19
CoV								0.130	0.141

Table 16
Collated numerical results totalling eight RHS-to-RHS X joints under brace in-plane bending, reported by Yu [19].

Specimen	b_0 (mm)	h_0 (mm)	t_0 (mm)	b_1 (mm)	h_1 (mm)	t_1 (mm)	f_{y0} (MPa)	θ_1 (°)	n	$2\gamma^*$	η^*	$M_{1u,ip}$ (kNm)	$M_{1u,ip}/M_{y,ip}$
x10ie05	150	150	10.00	150	75	10.00	355	90	0	15	0.5	37.1	1.34
x10ie	150	150	10.00	150	150	10.00	355	90	0	15	1.0	89.7	1.26
x10ie2	150	150	10.00	150	300	10.00	355	90	0	15	2.0	259.7	1.19
x11i	150	150	6.25	150	150	6.25	355	90	0	24	1.0	50.0	1.37
x11ie2	150	150	6.25	150	300	6.25	355	90	0	24	2.0	128.7	1.06
x12ie05	150	150	4.29	150	75	4.29	355	90	0	35	0.5	12.2	1.72
x12i	150	150	4.29	150	150	4.29	355	90	0	35	1.0	28.6	1.28
x12ie2	150	150	4.29	150	300	4.29	355	90	0	35	2.0	76.5	0.97

Table 17

Evaluation of design methods for the loading case of brace in-plane bending.

Specimen	f_{y0} (MPa)	2γ*	η*	$M_{1u,ip}$ (kNm)	$M_{1u,ip}/M_{C,M,ip}$	$M_{1u,ip}/M_{Yu,ip}$	$M_{1u,ip}/M_{Kuhn,ip}$	$M_{1u,ip}/M_{Lan,ip}$	$M_{1u,ip}/M_{P,M,ip}$	$M_{1u,ip}/M_{P,LK,ip}$
x10ie05	355	15	0.5	37.1	1.40	1.36	1.40	1.34	1.34	1.34
x10ie	355	15	1.0	89.7	1.33	1.25	1.32	1.26	1.33	1.34
x10ie2	355	15	2.0	259.7	1.25	1.24	1.25	1.19	1.39	1.41
x11i	355	24	1.0	50.0	1.63	1.24	1.64	1.37	1.63	1.65
x11ie2	355	24	2.0	128.7	1.25	1.18	1.26	1.15	1.39	1.41
x12ie05	355	35	0.5	12.2	2.48	1.38	2.48	1.84	2.23	2.22
x12i	355	35	1.0	28.6	1.84	1.11	1.84	1.54	1.84	1.82
x12ie2	355	35	2.0	76.5	1.40	1.29	1.40	1.40	1.55	1.54
Mean					1.57	1.25	1.57	1.39	1.59	1.59
CoV					0.265	0.072	0.265	0.159	0.198	0.191

Note: The material factor (C_f) equals 1.0 for all the joints.

Table 18
Effects of chord sidewall convexity and thickness tolerance on the resistance of RHS-to-RHS T joints under brace in-plane bending (Nagui [42])

Specimen	2γ	Steel grade	$M_{1u,ip}$ (kNm)	$M_{C,ip}$ (kNm)	$M_{1u,ip}/M_{C,ip}$
t12i (convexity: 1%)	35	S355	28.9	22.9	1.26
	35	S460	34.5	29.7	1.16
	35	S700	50.3	46.1	1.09
t12i* (convexity: 1% + thickness : -10%)	35	S355	24.7	22.9	1.08
	35	S460	29.7	29.7	1.00
	35	S700	43.2	46.1	0.94
t13i (convexity: 1%)	30	S355	37.2	27.2	1.37
	30	S460	44.7	36.4	1.22
	30	S700	64.8	55.4	1.17
t13i* (convexity: 1% + thickness : -10%)	30	S355	31.9	27.2	1.17
	30	S460	38.4	36.4	1.05
	30	S700	55.8	55.4	1.01
Mean					1.13
CoV					0.109

Table 19

Collated numerical results totalling eight RHS-to-RHS X joints under brace out-of-plane bending, reported by Yu [19].

Specimen	b_0 (mm)	h_0 (mm)	t_0 (mm)	b_1 (mm)	h_1 (mm)	t_1 (mm)	f_{y0} (MPa)	θ_1 (°)	n	$2\gamma^*$	η^*	$M_{1u,op}$ (kNm)	$M_{1u,op}/M_{y,op}$
x10oe05	150	150	10.00	150	75	10.00	355	90	0	15	0.5	80.4	1.29
x10oe	150	150	10.00	150	150	10.00	355	90	0	15	1.0	119.4	1.20
x10oe2	150	150	10.00	150	300	10.00	355	90	0	15	2.0	192.5	1.11
x11o	150	150	6.25	150	150	6.25	355	90	0	24	1.0	59.4	1.03
x11oe2	150	150	6.25	150	300	6.25	355	90	0	24	2.0	108.6	1.03
x12oe05	150	150	4.29	150	75	4.29	355	90	0	35	0.5	23.0	1.08
x12o	150	150	4.29	150	150	4.29	355	90	0	35	1.0	37.2	0.98
x12oe2	150	150	4.29	150	300	4.29	355	90	0	35	2.0	62.7	0.88

Table 20

Evaluation of design methods for the loading case of brace out-of-plane bending.

Specimen	f_{y0} (MPa)	$2\gamma^*$	η^*	$M_{1u,op}$ (kNm)	$M_{1u,op}/M_{C,M,op}$	$M_{1u,op}/M_{Yu,op}$	$M_{1u,op}/M_{Kuhn,op}$	$M_{1u,op}/M_{Lan,op}$	$M_{1u,op}/M_{P,M,op}$	$M_{1u,op}/M_{P,LK,op}$
x10oe05	355	15	0.5	80.4	1.36	1.21	1.36	1.29	1.29	1.29
x10oe	355	15	1.0	119.4	1.26	1.14	1.26	1.20	1.26	1.28
x10oe2	355	15	2.0	192.5	1.16	1.06	1.16	1.11	1.29	1.31
x11o	355	24	1.0	59.4	1.22	1.09	1.23	1.03	1.22	1.23
x11oe2	355	24	2.0	108.6	1.22	1.12	1.23	1.12	1.35	1.37
x12oe05	355	35	0.5	23.0	1.55	1.30	1.56	1.15	1.39	1.39
x12o	355	35	1.0	37.2	1.41	1.26	1.41	1.18	1.41	1.40
x12oe2	355	35	2.0	62.7	1.26	1.17	1.27	1.25	1.40	1.39
Mean					1.30	1.17	1.31	1.17	1.33	1.33
CoV					0.097	0.070	0.097	0.073	0.054	0.046

Note: The material factor (C_f) equals 1.0 for all the joints.

Table 21

Recommended design resistance for chord sidewall failure in RHS joints under brace axial compression using the modified bearing-buckling method.

<table>
<tr><td>RHS-to-RHS X, T and Y joints (class a)</td><td colspan="2">Brace axial compression loading</td></tr>
<tr><td rowspan="8">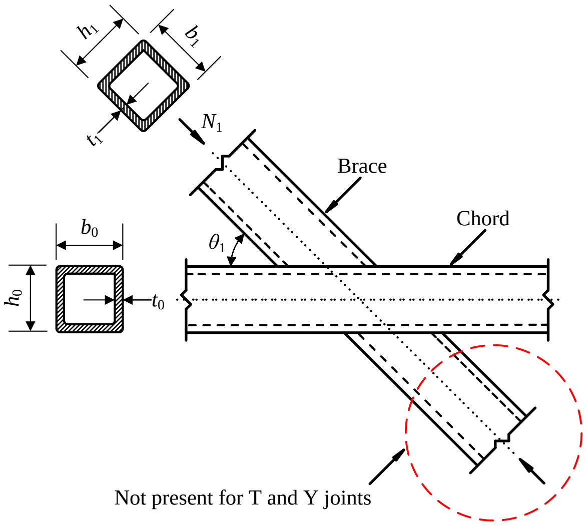
</td><td>$N_{1,\mathrm{Rd}} = C_\mathrm{f} f_\mathrm{k} t_0 \left(2h_1 + 10t_0\right)\sqrt{\frac{1}{\sin\theta_1}} Q_\mathrm{f}$</td><td>$f_\mathrm{k} = \chi_{0.5}\left(\frac{h_0}{h_1}\right)^{0.15} f_{y0} \leq f_{y0}$</td></tr>
<tr><td colspan="2">Parameters</td></tr>
<tr><td colspan="2">$C_\mathrm{f} = 1.1\text{-}0.1 f_{y0}/355 \leq 1.0$</td></tr>
<tr><td colspan="2">$\chi_{0.5}$ is the reduction factor for column buckling according to e.g., EN 1993-1-1 [6] using the buckling curve c, or an equivalent code/standard, and a normalised slenderness:
$$\lambda_{0.5} = \frac{1.73\left(\frac{h_0}{t_0} - 2\right)}{\pi\sqrt{\frac{E}{f_{y0}}}}$$</td></tr>
<tr><td colspan="2">$Q_\mathrm{f} = \left(1 - |n|\right)^{0.1}$ with n in the connecting chord face
$n = \frac{N_{0,\mathrm{Ed}}}{N_{\mathrm{pl},0,\mathrm{Rd}}} + \frac{M_{0,\mathrm{Ed}}}{M_{\mathrm{pl},0,\mathrm{Rd}}}$ for class 1 or 2 chord cross-sections under chord compression stress and for chord cross-sections under chord tension stress; $M_{\mathrm{el,Rd}}$ should be used for class 3 chord cross-sections.</td></tr>
<tr><td colspan="2">Validity ranges</td></tr>
<tr><td colspan="2">steel grades up to S960; β=1.0; $b_0/t_0 \leq 40$, $h_0/t_0 \leq 40$; $0.25 \leq h_1/h_0 \leq 2.0$; $0.5 \leq h_0/b_0 \leq 2.0$; $\theta_1 \geq 30°$.</td></tr>
<tr><td colspan="3">These recommendations may also be used for other X joints under brace axial compression:

(1) Plate-to-RHS X joints (use $t_1 = h_1$) and RHS-to-RHS X joints both with nominal $f_{y0} \leq 460$ MPa, β=1.0 and $h_1/h_0 \leq 0.25$, but use $f_\mathrm{k} = f_{y0}$.

(2) For X joints (class a) with an RHS brace welded to one side of the chord and supported by a flat plate or another profile welded to the opposite side of the chord, the lower effective h_1 on either side and $\lambda_{0.5}$ should be used for the determination of the resistance.

(3) For X joints (class b) with an RHS brace welded to one side of the chord and supported by a flat plate or another profile unwelded to the opposite side of the chord, the lower effective h_1 on either side and $\lambda_{0.7} = 1.4\lambda_{0.5}$ should be used for the determination of the resistance. Here, the chord cross-section slenderness should not exceed class 3.

(4) For other unspecified X joints (class c), the resistance should be determined using $\lambda_{1.0} = 2\lambda_{0.5}$.</td></tr>
<tr><td colspan="3">The cross-section slenderness of class 1, 2 and 3 is defined in national standards.</td></tr>
</table>

Table 22

Recommended design resistance for chord sidewall failure in RHS joints under brace axial compression using the Lan-Kuhn method.

<table>
<tr><td>RHS-to-RHS X, T and Y joints (class a)</td><td colspan="2">Brace axial compression loading</td></tr>
<tr><td rowspan="7">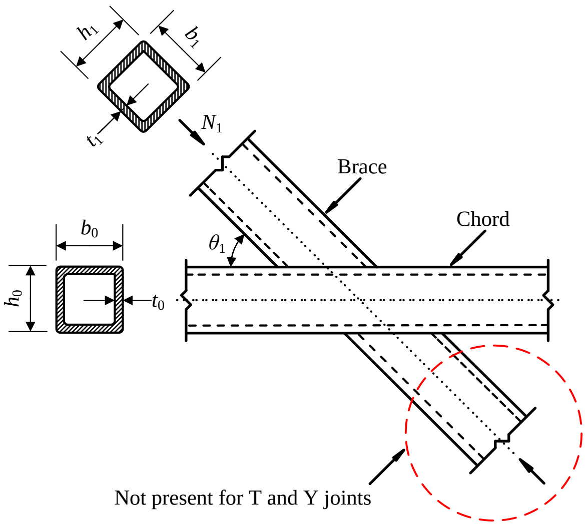
</td><td>$N_{1,\mathrm{Rd}} = C_\mathrm{f} f_\mathrm{k} t_0 \left(2h_1 + 10t_0\right) \sqrt{\dfrac{1}{\sin\theta_1}} Q_\mathrm{f}$</td><td>$f_\mathrm{k} = \chi_{0.5} \left(\dfrac{h_0}{h_1}\right)^{0.15} f_{y0} \le f_{y0}$</td></tr>
<tr><td colspan="2">Parameters</td></tr>
<tr><td colspan="2">$C_\mathrm{f} = 1.1\text{-}0.1 f_{y0}/355 \le 1.0$</td></tr>
<tr><td colspan="2">$\chi_{0.5}$ is the buckling reduction factor obtained from:
$\chi_{0.5} = 1.12\text{-}0.012 \dfrac{h_0}{t_0} \sqrt{\dfrac{f_{y0}}{355}}$</td></tr>
<tr><td colspan="2">$Q_\mathrm{f} = \left(1 - |n|\right)^{0.1}$ with n in connecting chord face
$n = \dfrac{N_{0,\mathrm{Ed}}}{N_{\mathrm{pl},0,\mathrm{Rd}}} + \dfrac{M_{0,\mathrm{Ed}}}{M_{\mathrm{pl},0,\mathrm{Rd}}}$ for class 1 or 2 chord cross-sections under chord compression stress and for chord cross-sections under chord tension stress; $M_{\mathrm{el,Rd}}$ should be used for class 3 chord cross-sections.</td></tr>
<tr><td colspan="2">Validity ranges</td></tr>
<tr><td colspan="2">steel grades up to S960; β=1.0; $b_0/t_0 \le 40$, $h_0/t_0 \le 40$; $0.25 \le h_1/h_0 \le 2.0$; $0.5 \le h_0/b_0 \le 2.0$; $\theta_1 \ge 30°$.</td></tr>
<tr><td colspan="3">These recommendations may also be used for other X joints under brace axial compression:

(1) Plate-to-RHS X joints (use $t_1=h_1$) and RHS-to-RHS X joints both with nominal $f_{y0} \le 460$ MPa, β=1.0 and $h_1/h_0 \le 0.25$, but use $f_\mathrm{k}=f_{y0}$.

(2) For X joints (class a) with an RHS brace welded to one side of the chord and supported by a flat plate or another profile welded to the opposite side of the chord, the lower effective h_1 on either side and $\chi_{0.5}$ should be used for the determination of the resistance.

(3) For X joints (class b) with an RHS brace welded to one side of the chord and supported by a flat plate or another profile unwelded to the opposite side of the chord, the lower effective h_1 on either side and $\chi_{0.7}$ should be used for the determination of the resistance. The $\chi_{0.7}$ value could be obtained from:
$\chi_{0.7} = 1.12\text{-}0.017 \dfrac{h_0}{t_0} \sqrt{\dfrac{f_{y0}}{355}}$
Here, the chord cross-section slenderness should not exceed class 3.

(4) For other unspecified X joints (class c), the resistance should be determined using $\lambda_{1.0}=2\lambda_{0.5}$, see Table 21.</td></tr>
<tr><td colspan="3">The cross-section slenderness of class 1, 2 and 3 is defined in national standards.</td></tr>
</table>